Laser cooling and trapping of atoms

H. J. Metcalf

Department of Physics, State University of New York, Stony Brook, New York 11794

P. van der Straten

Debye Institute, Department of Atomic- and Interface Physics, Utrecht University, P.O. Box 80.000, 3508 TA Utrecht, The Netherlands

Received August 27, 2002; revised manuscript received November 25, 2002

A review is presented of some of the principal techniques of laser cooling and trapping that have been developed during the past 20 years. Its approach is primarily experimental, but its quantitative descriptions are consistent in notation with most of the theoretical literature. It begins with a simplified introduction to optical forces on atoms, including both cooling and trapping. Then its three main sections discuss its three selected features, (1) quantization of atomic motion, (2) effects of the multilevel structure of atoms, and (3) the effects of polychromatic light. Each of these features is an expansion in a different direction from the simplest model of a classical, two-level atom moving in a monochromatic laser field.

OCIS codes: 020.7010, 300.6210.

1. INTRODUCTION

The combination of laser cooling and atom trapping has produced astounding new tools for atomic physicists.[1] These experiments require the exchange of momentum between atoms and an optical field, usually at a nearly resonant frequency. The energy of the light $\hbar\omega$ changes the internal energy of the atom, and the angular momentum $\hbar$ changes the orbital angular momentum ℓ of the atom, as described by the well-known selection rule $\Delta\ell = \pm 1$. By contrast, the linear momentum of the light $p = \hbar\omega/c$ ($\mathbf{p} = \hbar\mathbf{k}$) cannot change the internal atomic degrees of freedom and therefore must change the momentum of the atoms in the laboratory frame. The force resulting from this momentum exchange between the light field and the atoms can be used in many ways to control atomic motion and is the subject of this paper.

If the light is absorbed, the atom makes a transition to the excited state, and the return to the ground state can be either by spontaneous or by stimulated emission. The nature of the optical force that arises from these two different processes is quite different and will be described separately. The spontaneous emission case is different from the familiar quantum mechanical calculations that use state vectors to describe the state of the system, because spontaneous emission causes the state of the system to evolve from a pure state into a mixed state. Since spontaneous emission is an essential ingredient for the dissipative nature of the optical forces, the density matrix is needed to describe it.

A. Radiative Optical Forces

In the simplest case, the absorption of well-directed light from a laser beam, the momentum exchange between the light field and the atoms results in a force

$$\mathbf{F} = \mathrm{d}\mathbf{p}/\mathrm{d}t = \hbar\mathbf{k}\gamma_p, \tag{1}$$

where γ_p is the excitation rate of the atoms. The absorption leaves the atoms in their excited state, and, if the light intensity is low enough that they are much more likely to return to the ground state by spontaneous emission than by stimulated emission, the resulting fluorescent light carries off momentum $\hbar k$ in a random direction. The momentum exchange from the fluorescence averages zero, so the net total force is given by Eq. (1).

The scattering rate γ_p depends on the laser detuning from atomic resonance $\delta \equiv \omega_\ell - \omega_a$, where ω_ℓ is the laser frequency and ω_a is the atomic resonance frequency. This detuning is measured in the atomic reference frame, and it is necessary that the Doppler-shifted laser frequency in the moving atoms' reference frame be used to calculate the absorption and scattering rate. The excitation rate γ_p for a two-level atom is given by the Lorentzian

$$\gamma_p = \frac{s_0\gamma/2}{1 + s_0 + [2(\delta + \omega_D)/\gamma]^2}, \tag{2}$$

where $\gamma \equiv 1/\tau$ is an angular frequency corresponding to the decay rate of the excited state. Here $s_0 = I/I_s$ is the ratio of the light intensity I to the saturation intensity $I_s \equiv \pi hc/3\lambda^3\tau$, which is a few mW/cm^2 for typical atomic transitions. The Doppler shift seen by the moving atoms is $\omega_D = -\mathbf{k}\cdot\mathbf{v}$ (note that $\mathbf{k}$ opposite to $\mathbf{v}$ produces a positive Doppler shift). The force is thus velocity dependent, and the experimenter's task is to exploit this dependence to reach the desired goal, for example, optical friction for laser cooling.

The maximum attainable deceleration is obtained for very high light intensities. High-intensity light can produce faster absorption, but it also causes equally fast stimulated emission; the combination produces neither deceleration nor cooling. The momentum transfer to the atom in stimulated emission is in the direction opposite to what it was in absorption, resulting in a net transfer of

Table 1. Overview of Paper Contents

Section	Levels[a]	Frequencies	Motion	Dimensions	Topics
1					Forces and temperature
2	TLA	Single	Classical	1, 3	Beam slowing Molasses Optical traps
3	TLA	Single	Quantum	1, 3	Dark states and VSCPT Optical lattices
4	Multiple	Single	Classical	1	Sub-Doppler cooling Magneto-optical traps
5	TLA	Multiple	Classical	1	Bichromatic force Other polychromatic forces

[a] TLA, two-level atom.

zero. Since high intensity causes the atom to divide its time equally between ground and excited states, the force is limited to $\mathbf{F} = \hbar\mathbf{k}\gamma_p$; so the deceleration saturates at a value $\mathbf{a}_{\max} = \hbar\mathbf{k}\gamma/2M$ [see Eq. (2)].

B. Dipole Optical Forces

When the detuning $\delta \gg \gamma$, spontaneous emission may be much less frequent than stimulated emission. The dissipative radiative force found from Eqs. (1) and (2) is necessary for laser cooling, but the conservative dipole force arises from stimulated emission and derives from the gradient of the light shift.

To find the light shift, the dressed-atom picture provides the easiest description, and, for a single laser beam traveling in the $\hat{x}$ direction with Rabi frequency $\Omega = \gamma\sqrt{s_0/2}$, the light shift is given by

$$\omega_{ls} = (\sqrt{\Omega^2 + \delta^2} - \delta)/2. \tag{3}$$

For sufficiently large detuning $\delta \gg \Omega$, approximation of Eq. (3) leads to $\omega_{ls} \approx \Omega^2/4\delta = \gamma^2 s_0/8\delta$.

In a standing wave in one dimension with $\delta \gg \Omega$, the light shift $\omega_{ls}(x)$ varies sinusoidally from node to antinode, and also spontaneous emission is suppressed, so that $\hbar\omega_{ls}(x)$ may be treated as a potential $U(x)$. The resulting dipole force is

$$\mathbf{F}(x) = -\nabla U(x) = -\frac{\hbar\gamma^2}{8\delta I_s}\nabla I(x), \tag{4}$$

where $I(x)$ is the total intensity distribution of the standing-wave light field of period $\lambda/2$. For such a standing wave, the optical electric field (and the Rabi frequency) at the antinodes is double that of each traveling wave that composes it, and so the total intensity $I_{\max}$ at the antinodes is four times that of the single traveling wave.

C. Temperature

The idea of "temperature" in laser cooling requires some careful discussion and disclaimers. In thermodynamics, temperature is carefully defined as a parameter of the state of a closed system in thermal equilibrium with its surroundings. This, of course, requires that there be thermal contact, i.e., heat exchange, with the environment. In laser cooling this is clearly not the case, because a sample of atoms is always absorbing and scattering light. Furthermore, there is essentially no heat exchange (the light cannot be considered as heat even though it is indeed a form of energy). Thus the system may very well be in a steady-state situation but certainly not in thermal equilibrium, so that the assignment of a thermodynamic "temperature" is completely inappropriate.

Nevertheless, it is convenient to use the label of "temperature" to describe an atomic sample whose average kinetic energy $\langle E_k \rangle$ in one dimension has been reduced by the laser light, and this is written simply as $k_B T/2 = \langle E_k \rangle$, where k_B is Boltzmann's constant. It must be remembered that this temperature assignment is absolutely inadequate for atomic samples that do not have a Maxwell–Boltzmann velocity distribution, whether or not they are in thermal contact with the environment: There are infinitely many velocity distributions that have the same value of $\langle E_k \rangle$ but are so different from one another that characterizing them by the same temperature is a severe error. In the special case where there is a true damping force, $F \propto -v$, and where the diffusion in momentum space is a constant independent of momentum, solutions of the Fokker–Planck equation can be found analytically and lead to a Maxwell–Boltzmann distribution that does indeed have a temperature.

It is convenient to define a single dimensionless parameter $\varepsilon \equiv \omega_r/\gamma$ that is ubiquitous in describing laser cooling. It is the ratio of the recoil frequency $\omega_r \equiv \hbar k^2/2M$ to the natural width γ, and as such embodies most of the important information that characterizes laser cooling on a particular atomic transition. For atoms under consideration for laser cooling, ε is of the order of 10^{-3}–10^{-2}.

D. Organization of this Paper

This paper is organized as follows (see Table 1): After a broad introduction, the simplest case of optical forces on two-level atoms from a single-frequency light field is presented in Section 2. Several aspects of the classical motion of neutral atoms under these forces are introduced and discussed. These include beam slowing, optical molasses, and optical traps. With this as a basis, Sections 3–5 address cases where these simplifications are no longer valid:

- In Section 3 the phenomena associated with quantization of the atomic motion are considered. Atoms

are no longer regarded as point particles whose position and momentum can be simultaneously known to arbitrary precision, but instead they are described by wave functions that include their center-of-mass motion in the laboratory frame.

- In Section 4 the simplification of the two-level atom is lifted. Here the importance of light polarization and selection rules appear, and the concept of sub-Doppler cooling is described. Laser cooling is no longer limited by the natural decay rate γ, and atoms can be cooled all the way to the recoil limit $k_B T/2 = \hbar\omega_r$ determined by $\omega_r \ll \gamma$. The influence of magnetic fields becomes much more important than for the two-level case, and it not only allows the existence of the magneto-optical trap (MOT) but also leads to sub-Doppler temperatures.
- In Section 5 the extraordinarily large forces associated with polychromatic light are described. The radiative force is limited by the natural lifetime to $\hbar k\gamma_p$, and the velocity-dependent part of the Sisyphus force is similarly limited by γ. But multifrequency light, even on a two-level atom, can exert much stronger cooling forces, enabling smaller and more efficient beam slowing for trapping or other purposes.

Much of the material here was taken from our recent textbook,[1] and the reader is encouraged to consult that source for the origin of many of the formulas presented in the present paper, as well as for further reading and more detailed references to the literature.

2. OPTICAL FORCES ON TWO-LEVEL ATOMS

A. Slowing Atomic Beams

Among the earliest laser-cooling experiments was deceleration of atoms in a beam.[2] Phillips and Metcalf exploited the Doppler shift to make the momentum exchange (hence the force) velocity dependent. The approach worked by directing a laser beam opposite to an atomic beam so that the atoms could absorb light, and hence momentum $\hbar k$, very many times along their paths through the apparatus as shown in Fig. 1.[2,3] Of course, excited-state atoms cannot absorb light efficiently from the laser that excited them, so between absorptions they must return to the ground state by spontaneous decay, accompanied by emission of fluorescent light. The spatial symmetry of the emitted fluorescence results in an average of zero net momentum transfer from many such fluorescence events. Thus the net force on the atoms is in the direction of the laser beam, and the maximum deceleration is limited by the spontaneous emission rate γ.

Since the maximum deceleration $\mathbf{a}_{\max} = \hbar\mathbf{k}\gamma/2M$ is fixed by atomic parameters, it is straightforward to calculate the minimum stopping length $L_{\min}$ and time $t_{\min}$ for the rms velocity of atoms $\bar{v} = 2\sqrt{k_B T/M}$ at the source temperature. The result is $L_{\min} = \bar{v}^2/2a_{\max}$ and $t_{\min} = \bar{v}/a_{\max}$. In Table 2 are some of the parameters for slowing a few atomic species of interest from the peak of the thermal velocity distribution.

Maximizing the scattering rate γ_p requires $\delta = -\omega_D$ in Eq. (2). If δ is chosen for a particular atomic velocity in the beam, then, as the atoms slow down, their changing Doppler shift will take them out of resonance. They will eventually cease deceleration after their Doppler shift has been decreased by a few times the power-broadened width $\gamma' = \gamma\sqrt{1 + s_0}$, corresponding to Δv of a few times $v_c = \gamma'/k$. Although this Δv of a few m/s is considerably larger than the typical atomic recoil velocity $v_r = \hbar k/M$ of a few cm/s, it is still only a small fraction of the atoms' average thermal velocity $\bar{v}$, so that significant further cooling or deceleration cannot be accomplished.

To achieve deceleration that changes the atomic speeds by hundreds of m/s, it is necessary to maintain $(\delta + \omega_D) \ll \gamma$ by compensating such large changes of the Doppler shift. This can be done by changing ω_D, or δ through either ω_ℓ or ω_a. The two most common methods for maintaining this resonance are sweeping the laser frequency ω_ℓ along with the changing ω_D of the decelerating atoms,[4–6] or spatially varying the atomic resonance frequency with an inhomogeneous dc magnetic field to keep the decelerating atoms in resonance with the fixed frequency laser.[1,2,7]

The use of a spatially varying magnetic field to tune the atomic levels along the beam path was the first method to succeed in slowing atoms.[2] It works as long as the Zee-

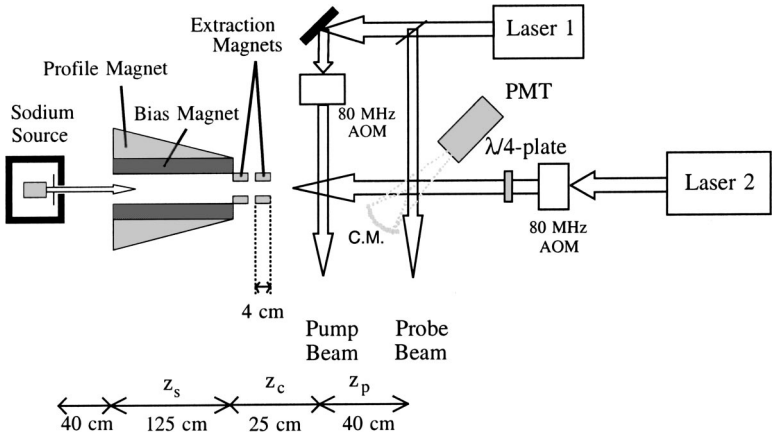

Fig. 1. Schematic diagram of apparatus for beam slowing. The tapered magnetic field is produced by layers of varying length on the solenoid.

Table 2. Parameters of Interest for Slowing Various Atoms[a]

Atom	T_{oven} (K)	$\bar{v}$ (m/s)	L_{min} (m)	t_{min} (ms)
H	1000	5000	0.012	0.005
He*	4	158	0.03	0.34
He*	650	2013	4.4	4.4
Li	1017	2051	1.15	1.12
Na	712	876	0.42	0.96
K	617	626	0.77	2.45
Rb	568	402	0.75	3.72
Cs	544	319	0.93	5.82

[a]The stopping length L_{min} and time t_{min} are minimum values. The oven temperature T_{oven} that determines the peak velocity is chosen to give a vapor pressure of 1 Torr. Special cases are H at 1000 K and He in the metastable triplet state, for which two rows are shown: one for a 4-K source and another for the typical discharge temperature.

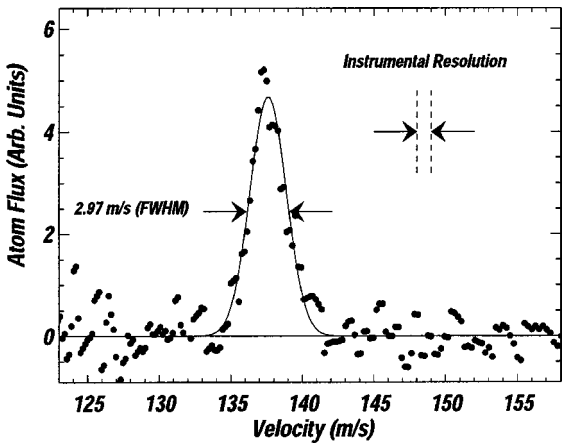

Fig. 2. The velocity distribution measured with the TOF method. The experimental width of approximately $\frac{1}{6}(\gamma/k)$ is shown by the dashed vertical lines between the arrows. The Gaussian fit through the data yields a FWHM of 2.97 m/s (from Ref. 9).

man shifts of the ground and excited states are different, so that the resonant frequency is shifted. The field can be tailored to provide the appropriate Doppler shift along the moving atom's path. A solenoid that can produce such a spatially varying field has layers of decreasing lengths. The technical problem of extracting the beam of slow atoms from the end of the solenoid can be simplified by reversing the field gradient and choosing a transition whose frequency decreases with increasing field.[8]

For alkali atoms such as sodium, a time-of-flight (TOF) method can be used to measure the velocity distribution of atoms in the beam. It employs two additional beams labeled pump and probe from laser 1 as shown in Fig. 1. Because these beams cross the atomic beam at 90°, $\omega_D = -\mathbf{k}\cdot\mathbf{v} = 0$, and the beams excite atoms at all velocities. The pump beam is tuned to excite and empty a selected ground hyperfine state (hfs), and it transfers more than 98% of the population as the atoms pass through its 0.5-mm width. To measure the velocity distribution of atoms in the selected hfs, this pump laser beam is interrupted for a period $\Delta t = 10$–$50\ \mu$s with an acoustic optical modulator (AOM). A pulse of atoms in the selected hfs passes the pump region and travels to the probe beam. The time dependence of the fluorescence induced by the probe laser, tuned to excite the selected hfs, gives the time of arrival, and this signal is readily converted to a velocity distribution. Figure 2 shows the measured velocity distribution of the atoms slowed by laser 2.

B. Optical Molasses

1. Doppler Cooling

It is straightforward to calculate the radiative force on atoms moving in a standing wave (counterpropagating laser beams) by using Eq. (2). In the low-intensity case, where stimulated emission is not important, the forces from the two light beams are simply added to give $\mathbf{F}_{\text{OM}} = \mathbf{F}_+ + \mathbf{F}_-$, where $\mathbf{F}_\pm$ are found from Eqs. (1) and (2). Then the sum of the two forces is

$$\mathbf{F}_{\text{OM}} \cong \frac{8\hbar k^2 \delta s_0 \mathbf{v}}{\gamma[1 + s_0 + (2\delta/\gamma)^2]^2} \equiv -\beta\mathbf{v}, \tag{5}$$

where terms of order $(kv/\gamma)^4$ and higher have been neglected. The slowing force is proportional to velocity for small enough velocities, resulting in viscous damping[10,11] that gives this technique the name optical molasses (OM).

These forces are plotted in Fig. 3. For $\delta < 0$, the sum of the forces opposes the velocity and therefore viscously damps the atomic motion. The force $\mathbf{F}_{\text{OM}}$ has maxima near $v \approx \pm\gamma\sqrt{s_0 + 1}/2k$ and decreases rapidly for larger velocities.

In laser cooling and related aspects of optical control of atomic motion, the forces arise because of the exchange of momentum between the atoms and the laser field. Since the energy and momentum exchange are necessarily in discrete quanta rather than continuous, the interaction is characterized by finite momentum kicks. This is often described in terms of steps in a fictitious space whose axes are momentum rather than position. These steps in momentum space are of size $\hbar k$ and thus are generally small compared with the magnitude of the atomic momenta at thermal velocities $\bar{v}$. This is easily seen by computing $\hbar k/M\bar{v} = \sqrt{T_r/T} \ll 1$.

If there were no other influence on the atomic motion, all atoms would quickly decelerate to $v = 0$, and the sample would reach $T = 0$, a clearly unphysical result. There is also some heating caused by the light beams that must be considered, and it derives from the discrete size of the momentum steps that the atoms undergo with each emission or absorption. Since the atomic momentum changes by $\hbar k$, their kinetic energy changes on average by at least the recoil energy $E_r = \hbar^2 k^2/2M = \hbar\omega_r$. This means that the average frequency of each absorption is $\omega_{\text{abs}} = \omega_a + \omega_r$, and the average frequency of each emission is $\omega_{\text{emit}} = \omega_a - \omega_r$. Thus the light field loses an average energy of $\hbar(\omega_{\text{abs}} - \omega_{\text{emit}}) = 2\hbar\omega_r$ for each scattering. This loss occurs at a rate $2\gamma_p$ (two beams), and the energy is converted to atomic kinetic energy because the atoms recoil from each event. The atomic sample is thereby heated because these recoils are in random directions.

The competition between this heating with the damping force of Eq. (5) results in a nonzero kinetic energy

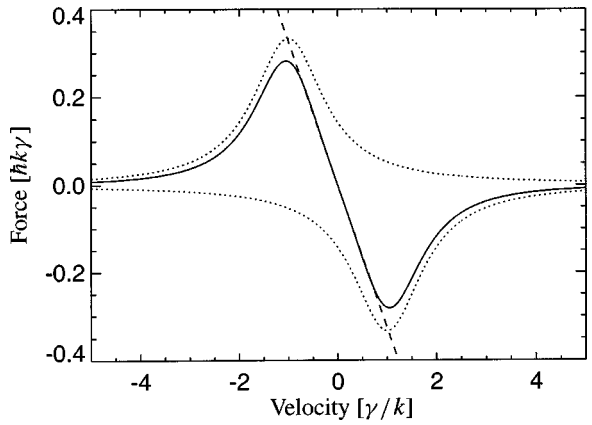

Fig. 3. Velocity dependence of the optical damping forces for 1D OM. The two dotted traces show the force from each beam, and the solid curve is their sum. The straight line shows how this force mimics a pure damping force over a restricted velocity range. These are calculated for $s_0 = 2$ and $\delta = -\gamma$, so there is some power broadening evident.

in steady state where the rates of heating and cooling are equal. Equating the cooling rate, $\mathbf{F}_{OM} \cdot \mathbf{v}$, to the heating rate, $4\hbar\omega_r\gamma_p$, the steady-state kinetic energy is $(\hbar\gamma/8)(2|\delta|/\gamma + \gamma/2|\delta|)$. This result is dependent on $|\delta|$, and it has a minimum at $2|\delta|/\gamma = 1$, whence $\delta = -\gamma/2$. The temperature found from the kinetic energy is then $T_D = \hbar\gamma/2k_B$, where k_B is Boltzmann's constant and T_D is called the Doppler temperature or the Doppler cooling limit. For ordinary atomic transitions, T_D is typically below 1 mK.

Another instructive way to determine T_D is to note that the average momentum transfer of many spontaneous emissions is zero, but the rms scatter of these about zero is finite. One can imagine these decays as causing a random walk in momentum space, similar to Brownian motion in real space, with step size $\hbar k$ and step frequency $2\gamma_p$, where the factor of 2 arises because of the two beams. The random walk results in an evolution of the momentum distribution as described by the Fokker–Planck equation, and it can be used for a more formal treatment of the laser-cooling process. It results in diffusion in momentum space with diffusion coefficient $D_0 \equiv 2(\Delta p)^2/\Delta t = 4\gamma_p(\hbar k)^2$. Then the steady-state temperature is given by $k_B T = D_0/\beta$. This turns out to be $\hbar\gamma/2$ as above for the case $s_0 \ll 1$ when $\delta = -\gamma/2$. This remarkable result predicts that the final temperature of atoms in OM is independent of the optical wavelength, atomic mass, and laser intensity (as long as it is not too large).

2. Atomic Beam Collimation—One Dimensional Optical Molasses—Beam Brightening

When an atomic beam crosses a one-dimensional (1D) OM as shown in Fig. 4, the transverse motion of the atoms is quickly damped, while the longitudinal component is essentially unchanged. This transverse cooling of an atomic beam is an example of a method that can actually increase its brightness [atoms/(sec sr cm^2)] because such active collimation uses dissipative forces to compress the phase-space volume occupied by the atoms. By contrast, the usual focusing or collimation techniques for light beams and most particle beams is restricted to selection by apertures or conservative forces that preserve the phase-space density of atoms in the beam.

This velocity compression at low intensity in one dimension can be simply estimated for two-level atoms to be approximately $v_c/v_D = \sqrt{\gamma/\omega_r} = \sqrt{1/\varepsilon}$. Here v_D is the velocity associated with the Doppler limit for laser cooling discussed below: $v_D = \sqrt{\hbar\gamma/2M}$. For Rb, $v_D = 12$ cm/s, $v_c = \gamma/k \simeq 4.6$ m/s, $\omega_r \simeq 2\pi \times 3.8$ kHz, and $1/\varepsilon \simeq 1600$. Including two transverse directions along with the longitudinal slowing and cooling discussed above, the decrease in phase-space volume from the momentum contribution alone for laser cooling of a Rb atomic beam can exceed 10^6. Clearly optical techniques can create atomic beams enormously more times intense than ordinary thermal beams, and also many orders of magnitude brighter.

3. Experiments in Three-Dimensional Optical Molasses

By use of three intersecting orthogonal pairs of oppositely directed beams, the movement of atoms in the intersection region can be severely restricted in all three dimensions, and many atoms can thereby be collected and cooled in a small volume.

Even though atoms can be collected and cooled in the intersection region, it is important to stress that this is *not* a trap. That is, atoms that wander away from the center experience no force directing them back. They are allowed to diffuse freely and even escape, as long as there is enough time for their very slow diffusive movement to allow them to reach the edge of the region of the intersection of the laser beams. Because the atomic velocities are randomized during the damping time $M/\beta = 2/\omega_r$, atoms execute a random walk in position space with a step size of $2v_D/\omega_r = \lambda/(\pi\sqrt{2\varepsilon}) \cong$ few μm. To diffuse a distance of 1 cm requires $\sim 10^7$ steps or ~ 30 s (Refs. 13 and 14).

Three-dimensional (3D) OM was first observed in 1985.[11] Preliminary measurements of the average kinetic energy of the atoms were done by blinking off the laser beams for a fixed interval. Comparison of the brightness of the fluorescence before and after the turnoff was used to calculate the fraction of atoms that left the region while it was in the dark. The dependence of this fraction on the duration of the dark interval was used to

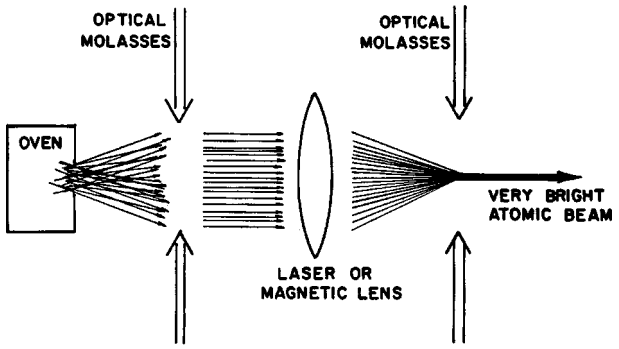

Fig. 4. Scheme for optical brightening of an atomic beam. First the transverse velocity components of the atoms are damped out by an OM, then the atoms are focused to a spot, and finally the atoms are recollimated in a second OM (from Ref. 12).

estimate the velocity distribution and hence the temperature. This method, which is usually referred to as release and recapture, is specifically designed to measure the temperature of the atoms, since the usual way of measuring temperatures cannot be applied to an atomic cloud of a few million atoms. The result was consistent with T_D as calculated from the Doppler theory, as described in Subsection 2.B.1.

Later a more sensitive ballistic technique was devised at the National Institute of Standards and Technology[15] (NIST) that showed the astounding result that the temperature of the atoms in OM was very much lower than T_D. These experiments also found that OM was less sensitive to perturbations and more tolerant of alignment errors than was predicted by Doppler theory. For example, if the intensities of the two counterpropagating laser beams forming an OM were unequal, then the force on atoms at rest would not vanish, but the force on atoms with some nonzero drift velocity *would* vanish. This drift velocity can be easily calculated by using unequal intensities s_{0+} and s_{0-}, to derive an analog of relation (5). Thus atoms would drift out of an OM, and the calculated rate would be much faster than observed when the beams were deliberately unbalanced in the experiments.[16]

It was an enormous surprise to observe that the ballistically measured temperature of the Na atoms[15] was as much as 10 times *lower* than $T_D = 240\ \mu$K, the temperature minimum calculated from the theory. This breaching of the Doppler limit forced the development of an entirely new picture of OM that accounts for the fact that in three dimensions a two-level picture of atomic structure is inadequate. The multilevel structure of atomic states, and optical pumping among these sublevels, must be considered in the description of 3D OM, as discussed in Subsection 4.B.5.

C. Dipole Force Optical Traps

1. Single-Beam Optical Traps for Two-Level Atoms

The simplest imaginable trap consists of a single, strongly focused Gaussian laser beam[17,18] (see Fig. 5) whose intensity at the focus varies transversely with r as

$$I(r) = I_0 \exp(-r^2/w_0^2), \tag{6}$$

where w_0 is the beam waist size. Such a trap has a well-studied and important macroscopic classical analog in a phenomenon called optical tweezers.[19–21]

With the laser light tuned below resonance ($\delta < 0$), the ground-state light shift is everywhere negative, but largest at the center of the Gaussian beam waist. Ground-state atoms therefore experience a force attracting them toward this center given by the gradient of the light shift, which is found from Eq. (3) and for $\delta/\gamma \gg s_0$ is given by Eq. (4). For the Gaussian beam, this transverse force at the waist is harmonic for small r and is given by

$$F \simeq \frac{\hbar\gamma^2}{4\delta}\frac{I_0}{I_s}\frac{r}{w_0^2}\exp(-2r^2/w_0^2) \tag{7}$$

In the longitudinal direction there is also an attractive force, but it is more complicated and depends on the details of the focusing. Thus this trap produces an attractive force on atoms in three dimensions.

Although it may appear that the trap does not confine atoms longitudinally because of the radiation pressure along the laser beam direction, careful choice of the laser parameters can indeed produce trapping in three dimensions. This can be accomplished because the radiation pressure force decreases as $1/\delta^2$ [see Eq. (2)], but, by contrast, the dipole force only decreases as $1/\delta$ for $\delta \gg \Omega$ [see Eq. (3)]. If $|\delta|$ is chosen to be sufficiently large, atoms spend very little time in the untrapped (actually repelled) excited state because its population is proportional to $1/\delta^2$. Thus a sufficiently large value of $|\delta|$ both produces longitudinal confinement and maintains the atomic population primarily in the trapped ground state.

The first optical trap was demonstrated in Na with light detuned below the D lines.[18] With 220 mW of dye laser light tuned ~650 GHz below the atomic transition and focused to a ~10-μm waist, the trap depth was $\sim 15\hbar\gamma$, corresponding to 7 mK. Single-beam dipole force traps can be made with the light detuned by a significant fraction of its frequency from the atomic transition. Such a far-off-resonance trap (FORT) was developed for Rb atoms by use of light detuned by nearly 10% to the red of the D_1 transition at $\lambda = 795$ nm (Ref. 22). Between 0.5 and 1 W of power was focused to a spot about 10 μm in size, resulting in a trap 6 mK deep where the light scattering rate was only a few hundred per second. The trap lifetime was more than half a second.

There is a qualitative difference when the trapping light is detuned by a large fraction of the optical frequency. In one such case, Nd:YAG light at $\lambda = 1064$ nm was used to trap Na, whose nearest transition is at $\lambda = 596$ nm (Ref. 23). In a more extreme case, a trap using $\lambda = 10.6\ \mu$m light from a CO_2 laser was used to trap Cs, whose optical transition is at a frequency ~12 times higher[24] ($\lambda = 852$ nm). For such large values of $|\delta|$, calculations of the trapping force cannot exploit the rotating-wave approximation as was done for Eq. (3), and the atomic behavior is similar to that in a dc field. It is important to remember that for an electrostatic trap Earnshaw's theorem precludes a field maximum, but that in this case there is indeed a local 3D intensity maximum of the focused light because it is not static.

2. Blue-Detuned Optical Traps

One of the principle disadvantages of the optical traps discussed above is that the negative detuning attracts atoms to the region of highest light intensity. This results in significant spontaneous emission unless the detuning is a large fraction of the optical frequency, such as in the Nd:YAG laser trap[23] or the CO_2 laser trap.[24] More important in some cases is that the trap relies on Stark shifting of the atomic energy levels by an amount equal to the trap depth, and this severely compromises the capabilities for precision spectroscopy in a trap.[25]

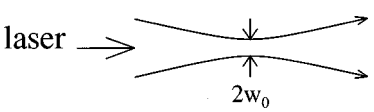

Fig. 5. A single focused laser beam produces the simplest type of optical trap.

Attracting atoms to the region of *lowest* intensity would ameliorate both of these concerns, but such a trap requires positive detuning (blue), and an optical configuration having a dark central region. One of the first experimental efforts at a blue-detuned trap used the repulsive dipole force to support Na atoms that were otherwise confined by gravity in an optical cup.[26] Two rather flat, parallel beams detuned by 25% of the atomic resonance frequency were directed horizontally and oriented to form a V-shaped trough. Their Gaussian beam waists formed a region ≃1 mm long where the potential was deepest, and hence provided confinement along their propagation direction as shown in Fig. 6. The beams were the $\lambda = 514$ nm and $\lambda = 488$ nm from an Ar laser, and the choice of two frequencies was not simply to exploit the full power of the multiline Ar laser, but also to avoid the spatial interference that would result from use of a single frequency.

Obviously a hollow laser beam would also satisfy the requirement for a blue-detuned trap, but conventional textbook wisdom shows that such a beam is not an eigenmode of a laser resonator.[27] Some lasers can make hollow beams, but these are illusions because they consist of rapid oscillations between the TEM_{01} and TEM_{10} modes of the cavity. Nevertheless, Maxwell's equations permit the propagation of such beams, and in the recent past there have been studies of the LaGuerre–Gaussian modes that constitute them.[28–30] The several ways of generating such hollow beams have been tried by many experimental groups and include phase and amplitude holograms, hollow waveguides, axicons or related cylindrical prisms, stressing fibers, and simply mixing the TEM_{01} and TEM_{10} modes with appropriate cylindrical lenses.

An interesting experiment was performed by using the ideas of Sisyphus cooling (see Subsection 4.B) with evanescent waves combined with a hollow beam formed with an axicon.[31] In the previously reported experiments with atoms bouncing under gravity from an evanescent wave field,[32,33] they were usually lost to horizontal motion for several reasons, including slight tilting of the surface, surface roughness, horizontal motion associated with their residual motion, and horizontal ejection by the Gaussian profile of the evanescent wave laser beam. The authors of Ref. 31 simply confined their atoms in the horizontal direction by surrounding them with a wall of blue-detuned light in the form of a vertical hollow beam. Their gravito-optical surface trap cooled Cs atoms to ≃3 μK at a density of $\simeq 3 \times 10^{10}$ cm^{-3} in a sample whose $1/e$ height in the gravitational field was only 19 μm. Simple ballistics gives a frequency of 450 bounces/s, and the ≃6-s lifetime (limited only by background gas collisions) corresponds to several thousand bounces. However, at such low energies the de Broglie wavelength of the atoms is ≃1/4 μm, and the atomic motion is no longer accurately described classically, but requires de Broglie wave methods.

3. QUANTUM STATES OF MOTION

As the techniques of laser cooling advanced from a laboratory curiosity to a tool for new problems, the emphasis shifted from attaining the lowest possible steady-state temperatures to the study of elementary processes, especially the quantum mechanical description of the atomic motion. In the completely classical description of laser cooling, atoms were assumed to have well-defined position and momentum that could be known simultaneously with arbitrary precision. However, when atoms are moving sufficiently slowly that their de Broglie wavelength precludes their localization to less than $\lambda/2\pi$, these descriptions fail and a quantum mechanical description is required. Such exotic behavior for the motion of whole atoms, as opposed to electrons in the atoms, was not considered before the advent of laser cooling simply because it is too far out of the range of ordinary experiments. A series of experiments in the early 1990s provided dramatic evidence for these new quantum states of motion of neutral atoms and led to the debut of de Broglie wave atom optics.

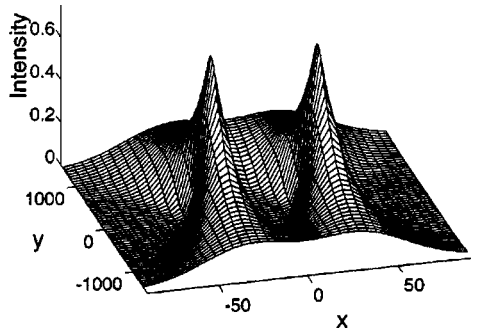

Fig. 6. Light intensity experienced by an atom located in a plane 30 μm above the beam waists of two quasi-focused sheets of light traveling parallel and arranged to form a V-shaped trough. The x and y dimensions are in micrometers (from Ref. 26).

The quantum description of atomic motion requires that the energy of such motion be included in the Hamiltonian. The total Hamiltonian for atoms moving in a light field would then be given by

$$\mathcal{H} = \mathcal{H}_{\text{atom}} + \mathcal{H}_{\text{rad}} + \mathcal{H}_{\text{int}} + \mathcal{H}_{\text{kin}}, \tag{8}$$

where $\mathcal{H}_{\text{atom}}$ describes the motion of the atomic electrons and gives the internal atomic energy levels, $\mathcal{H}_{\text{rad}}$ is the energy of the radiation field and is of no concern here because the field is not quantized, $\mathcal{H}_{\text{int}}$ describes the excitation of atoms by the light field and the concomitant light shifts, and $\mathcal{H}_{\text{kin}}$ is the kinetic energy operator of the motion of the atoms' center of mass. This Hamiltonian has eigenstates of not only the internal energy levels and the atom–laser interaction that connects them, but also of the kinetic energy operator $\mathcal{H}_{\text{kin}} \equiv P^2/2M$. These eigenstates will therefore be labeled by quantum numbers of the atomic states as well as the center-of-mass momentum p. Here and in the remainder of this section the momentum is measured in units of $\hbar k$. An atom in the ground state, $|g; p\rangle$, has an energy $E_g + p^2\hbar\omega_r$, which can take on a range of values. Here the kinetic energy of the atom is given in terms of the recoil frequency $\omega_r \equiv \hbar k^2/2M$.

Bose–Einstein condensation (BEC) is another example of atomic motion in the quantum domain. It occurs in the absence of light, and its onset is characterized by cooling to the point where the atomic de Broglie wavelengths

are comparable with the interatomic spacing. The topics discussed here concern the properties of cold atoms in an optical field, where the atomic de Broglie wavelengths are comparable with the optical wavelength λ.

A. Dark States

One special area of interest is the study of dark states, atomic states that cannot be excited by the light field. Some atomic states are trivially dark; that is, they cannot be excited because the light has the wrong frequency or polarization. The more interesting cases are superposition states created by coherent optical Raman coupling. A very special case are those superpositions whose excitable component vanishes exactly when their external (de Broglie wave) states are characterized by a particular momentum. Such velocity-selective coherent population trapping (VSCPT) has been a subject of considerable interest since its first demonstration in 1988.[34] VSCPT enables arbitrarily narrow momentum distributions and hence arbitrarily large delocalization for atoms in the dark states.[35] Adequate discussion of VSCPT requires a quantum mechanical description of the atomic motion.

1. VSCPT in Two-Level Atoms

To see how the quantization of the motion of a two-level atom in a monochromatic field allows the existence of a velocity-selective dark state, consider the states of a two-level atom with single internal ground and excited levels, $|g; p\rangle$ and $|e; p'\rangle$.

Two ground eigenstates $|g; p\rangle$ and $|g; p''\rangle$ are only coupled to one another by an optical field in certain special cases. For example, in a single pair of counterpropagating light beams there can be absorption-stimulated emission cycles that connect $|g; p\rangle$ to itself or to $|g; p \pm 2\rangle$, depending on whether the stimulated emission is induced by the beam that excited the atom or by the counterpropagating one. In the first case the states of the atom and field are left unchanged, but the interaction shifts the internal atomic energy levels, thereby producing the light shift. In the second case the initial and final kinetic energies of the atom differ by $\pm 4(p \pm 1)\hbar\omega_r$, so energy conservation requires $p = \mp 1$ (the energy of the light field is unchanged by the interaction, since all the photons in the field have energy $\hbar\omega_\ell$). Thus energy conservation corresponds to Raman resonance between the distinct states $|g; -1\rangle$ and $|g; +1\rangle$ and is therefore velocity selective.

The coupling of these two degenerate states by the light field produces off-diagonal matrix elements of the total Hamiltonian $\mathcal{H}$ of Eq. (8), and subsequent diagonalization of it results in the new ground eigenstates of $\mathcal{H}$ given by (see Fig. 7).

$$|\pm\rangle \equiv (|g;\ -1\rangle \pm |g;\ +1\rangle)/\sqrt{2}. \tag{9}$$

The excitation rate of the eigenstates $|\pm\rangle$ given in Eq. (9) to $|e; 0\rangle$ is proportional to the square of the electric dipole matrix element $\boldsymbol{\mu}$ given by

$$|\langle e;\ 0|\boldsymbol{\mu}|\pm\rangle|^2 = |\langle e;\ 0|\boldsymbol{\mu}|g;\ -1\rangle \pm \langle e;\ 0|\boldsymbol{\mu}|g;\ +1\rangle|^2/2. \tag{10}$$

This vanishes for $|-\rangle$ because the two terms on the right-hand side of Eq. (10) are equal, since $\boldsymbol{\mu}$ does not operate on the external momentum of the atom (dotted line of Fig. 7).

Excitation of $|\pm\rangle$ to $|e;\ \pm 2\rangle$ is much weaker, since it is off resonance because its energy is higher by $4\hbar\omega_r$, so that the required frequency is higher than to $|e; 0\rangle$. The resultant detuning is $4\omega_r = 8\varepsilon(\gamma/2)$, and for $\varepsilon = 0.22$, the value for the $2\ ^3S \rightarrow 3\ ^3P$ transition in He* used in our experiments,[36] this is large enough to reduce the excitation rate, making $|-\rangle$ semidark. Excitation to any state other than $|e;\ \pm 2\rangle$ or $|e; 0\rangle$ is forbidden by momentum conservation. Atoms are therefore optically pumped into the dark state $|-\rangle$, where they stay trapped, and since their momentum components are fixed, the result is VSCPT.

2. Another View of VSCPT

A useful view of this dark state can be obtained by considering that its components $|g;\ \pm 1\rangle$ have well-defined momenta and are therefore completely delocalized. Thus they can be viewed as waves traveling in opposite directions but having the same frequency, and therefore they form a standing de Broglie wave. The fixed spatial phase of this standing wave relative to the optical standing wave formed by the counterpropagating light beams results in the vanishing of the spatial integral of the dipole transition matrix element so that the state cannot be excited. This view can also help to explain the consequences of p not exactly equal to ± 1, where the de Broglie wave would be slowly drifting in space with respect to the standing wave of light. It is common to label the average of the momenta of the coupled states as the family momentum, $\mathcal{P}$, and to say that these states form a *closed family*, having family momentum $\mathcal{P} = 0$ (Refs. 34 and 37).

3. Bragg Diffraction and VSCPT

A completely new view of VSCPT has emerged from more careful consideration of the motion of such dark-state atoms in the spatially periodic field of oppositely propagating light beams.[38] This is Bragg diffraction, where the radiation field forms a periodic structure from which de Broglie waves are diffracted instead of vice versa. Here the de Broglie matter wave is Bragg reflected by the spatially periodic optical field: Matter and field have been

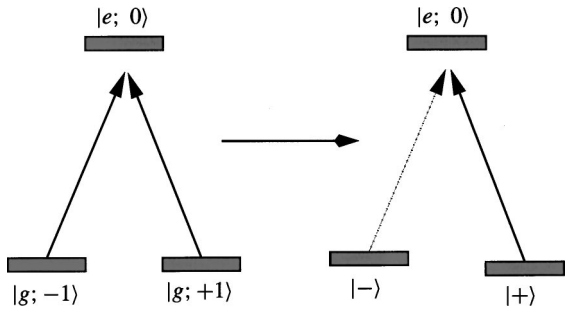

Fig. 7. Schematic diagram of the transformation of the eigenfunctions from the internal atomic states $|g; p\rangle$ to the eigenstates $|\pm\rangle$. The coupling between the two states $|g; p\rangle$ and $|g; p''\rangle$ by Raman transitions mixes them, and since they are degenerate, the eigenstates of $\mathcal{H}$ are the nondegenerate states $|\pm\rangle$.

interchanged from the usual case of Bragg reflection of an electromagnetic field by crystalline planes of atoms!

The usual case of x-ray Bragg reflection can be viewed as arising from multicenter scattering of radiation by atoms at each lattice site in a crystal. It follows that propagation of the reflected wave can occur only in the preferred direction. Such waves are the only ones not diffusively scattered by atoms in the lattice. The equivalent view of atoms in dark states is simply that the de Broglie wave fields propagate without scattering (i.e., no spontaneous emission) in the light field only when the atoms are indeed in dark states.

4. Case When $\mathcal{P}$ is Not Exactly 0

Since the momenta of the constituents of the eigenstates $|\pm\rangle$ must differ by ± 2, the states are not degenerate when the momenta are not exactly ± 1. Their superposition is therefore not a stationary state of the Hamiltonian in Eq. (8), so atoms escape because $|-\rangle$ will eventually evolve into $|+\rangle$. The rate for this evolution can be calculated from the Hamiltonian of Eq. (8) for the three-level system of one excited and two ground states. In the basis $|\pm(\mathcal{P})\rangle \equiv [|g;\ \mathcal{P}-1\rangle \pm |g;\ \mathcal{P}+1\rangle]/\sqrt{2}$ and $|e;\ \mathcal{P}\rangle$, this matrix has off-diagonal elements given by

$$\langle \pm(\mathcal{P})|\mathcal{H}_{\rm kin}| \mp (\mathcal{P})\rangle = 2\hbar\omega_r\mathcal{P}, \tag{11}$$

where $2\omega_r\mathcal{P} = \omega_D$ is the Doppler shift associated with the average momentum $\mathcal{P}$ of the ground states' constituents. The states $|g;\ -1\rangle$ and $|g;\ +1\rangle$ are just these basis states with $\mathcal{P} = 0$. Thus $|-(\mathcal{P})\rangle$ is coupled to $|+(\mathcal{P})\rangle$ by the atomic motion unless $\mathcal{P} = 0$.

The spontaneous decay of $|e;\ \mathcal{P}\rangle$ is modeled by making its energy complex, and so the three eigenvalues of $\mathcal{H}$ are all complex as a result of the mixing. The imaginary parts of the eigenvalues (decay rates) depend on $\mathcal{P}$, and one of them vanishes at $\mathcal{P} = 0$, corresponding to the VSCPT state. This state is called NC for noncoupled, and near $\mathcal{P} = 0$ its decay rate is[39,40]

$$\Gamma_{\rm NC} = (\gamma s_0/2)[1 - \sqrt{1 - [\mathcal{P}/\mathcal{P}_0]^2}], \tag{12}$$

where $\mathcal{P}_0 \equiv s_0/8\varepsilon$ (if $\mathcal{P} > \mathcal{P}_0$, then $\Gamma_{\rm NC} = \gamma s_0/2$). With $\varepsilon \equiv \omega_r/\gamma \approx 0.22$, we find $\mathcal{P}_0 \sim s_0/2$.

5. VSCPT in Real Atoms

Real atoms have multiple internal levels that include the effects of the magnetic, hyperfine, and other sublevels. The most well-studied example occurs in metastable He on the $2\ ^3S \rightarrow 2\ ^3P$ transition at $\lambda = 1.083\ \mu$m, using the $J = 1 \rightarrow 1$ component in counterpropagating beams of opposite circular polarization.[34] Decay from the excited $M_J = 0$ state to the ground $M_J = 0$ state is forbidden by the selection rules, so the ground $M_J = 0$ state is emptied by optical pumping, and the only populated ground states are $M_J = \pm 1$. Then the $\Delta M_J = \pm 1$ transitions can populate only the excited $M_J = 0$ state, thus forming a Λ system of levels.

The two ground states having $M_J = \pm 1$ can be coupled by a Raman transition requiring the participation of *both* light beams, and thus their momenta must be different by ± 2 in units of $\hbar k$. For the case where the σ^+ (σ^-) beam propagates in the positive (negative) z direction, the superposition states are given by

$$|\pm\rangle = [|g_{-1};\ -1\rangle \pm |g_{+1};\ +1\rangle]/\sqrt{2}, \tag{13}$$

where the subscripted quantum number denotes M_J and the other number denotes the atomic momentum. As for the two-level atom case discussed above, one of the states given in Eq. (13) is dark.

Unlike the usual cases of laser cooling, there is no damping force in this most commonly studied case of VSCPT because the Doppler and polarization gradient cooling cancel each other as a result of a numerical accident for this particular $J = 1 \rightarrow 1$ case. Thus atoms execute a random walk in momentum space until spontaneous emission lands them in the dark state of Eq. (13). Atoms that diffuse too far from $\mathcal{P} = 0$ are lost from the process. By contrast, in the two-level atom experiment[36] there is strong Doppler cooling because $2\ ^3S_1 \rightarrow 3\ ^3P_2$ is a $J = 1 \rightarrow 2$ transition, and this numerical accident does not occur. Moreover, Doppler cooling on this transition is very effective because the large value of ε makes the Doppler cooling limit $T_D = \hbar\gamma/2k_B \approx 36\ \mu$K, not very different from $T_r \approx 32\ \mu$K.

6. Entangled States

One of the most interesting aspects of dark-state physics arises from the entanglement of motional and internal states. This leads to the opportunity for fundamental studies of many topics whose basis is at the heart of quantum mechanics, such as the well-known Einstein–Podolsky–Rosen paradox, Schrödinger's cat, quantum communications, and quantum computing.[41,42] The key feature of entangled states is embodied in the form of Eq. (13). Here $|\pm\rangle$ is written as a sum of products, and it can be shown that is not possible to find a basis where this state can be described as an outer product.

Clearly dark-state entanglements with multilevel neutral atoms offer several advantages over related optical experiments. First, atoms arrive as discrete objects, unlike optical fields with the notorious difficulties of producing Fock states. Perhaps more important, the number of Hilbert spaces that are available, as well as their dimensionality, can each be larger than two.

A quantum-controlled NOT gate can be realized directly with the states that are entangled in VSCPT. This is because two independent Hilbert spaces, the external motion and the internal M_J levels, are entangled in the state. Therefore a measurement of one determines the other. This neutral atomic beam version of a controlled NOT gate is complementary to one realizable with trapped ions while retaining the relatively high isolation from environmental decoherence (the momentum states are naturally very robust, and the internal states are composed entirely of ground levels).

B. Optical Lattices

1. Introduction

In 1968 V. S. Letokhov[43] suggested that it is possible to confine atoms in the wavelength size regions of a standing wave by means of the dipole force that arises from the light shift. This was first accomplished in 1987 in one dimension with an atomic beam traversing an intense standing wave.[44] Since then the study of atoms confined in wavelength-size potential wells has become an impor-

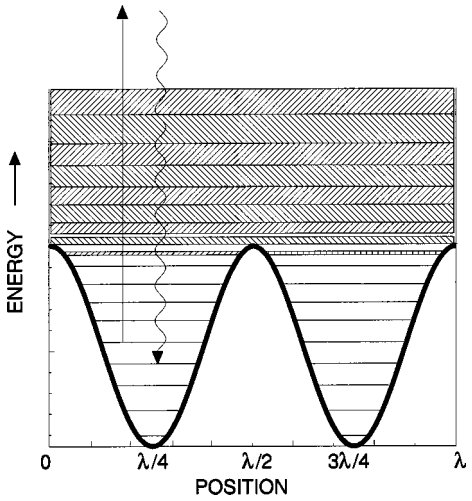

Fig. 8. Energy levels of atoms moving in the periodic potential of the light shift in a standing wave. There are discrete bound states deep in the wells that broaden at higher energy and become bands separated by forbidden energies above the tops of the wells. Under conditions appropriate to laser cooling, optical pumping among these states favors populating the lowest ones as indicated schematically by the arrows.

tant topic in optical control of atomic motion because it opens up configurations previously accessible only in condensed-matter physics using crystals.

The limits of laser cooling discussed in Subsection 4.B.5 suggest that atomic momenta can be reduced to a "few" times $\hbar k$. This means that their de Broglie wavelengths are equal to the optical wavelengths divided by a "few". If the depth of the optical potential wells is high enough to contain such very slow atoms, then their motion in potential wells of size $\lambda/2$ must be described quantum mechanically, since they are confined to a space of size comparable with their de Broglie wavelengths. Thus they do not oscillate in the sinusoidal wells as classical localizable particles, but instead occupy discrete, quantum mechanical bound states,[45] as shown in the lower part of Fig. 8.

The basic ideas of the quantum mechanical motion of particles in a periodic potential were laid out in the 1930s with the Kronig–Penney model and Bloch's theorem, and optical lattices offer important opportunities for their study. For example, these lattices can be made essentially free of defects with only moderate care in spatially filtering the laser beams to assure a single transverse mode structure. Furthermore, the shape of the potential is exactly known, and doesn't depend on the effect of the crystal field or the ionic energy level scheme. Finally, the laser parameters can be varied to modify the depth of the potential wells without changing the lattice vectors, and the lattice vectors can be changed independently by redirecting the laser beams. The simplest optical lattice to consider is a 1D pair of counterpropagating beams of the same polarization, as was used in the first experiment.[44]

Of course, such tiny traps are usually very shallow, so loading them requires cooling to the microkelvin regime. Even atoms whose energy exceeds the trap depth must be described as quantum mechanical particles moving in a periodic potential that display energy band structure.[45] Such effects have been observed in very careful experiments.

Atoms trapped in wavelength-sized spaces occupy vibrational levels similar to those of molecules. The optical spectrum can show Raman-like sidebands that result from transitions among the quantized vibrational levels[46,47] as shown in Fig. 9. These quantum states of atomic motion can also be observed by stimulated emission[46,48] and by direct rf spectroscopy.[49,50]

2. Properties of 3D Lattices

The name "optical lattice" is used rather than optical crystal because the filling fraction of the lattice sites is typically only a few percent (as of 1999). The limit arises because the loading of atoms into the lattice is typically done from a sample of trapped and cooled atoms, such as a MOT for atom collection, followed by an optical molasses for laser cooling. The atomic density in such experiments is limited to a few times $10^{11}/\mathrm{cm}^3$ by collisions and multiple light scattering. Since the density of lattice sites of size $\lambda/2$ is a few times $10^{13}/\mathrm{cm}^3$, the filling fraction is necessarily small. With the advent of experiments

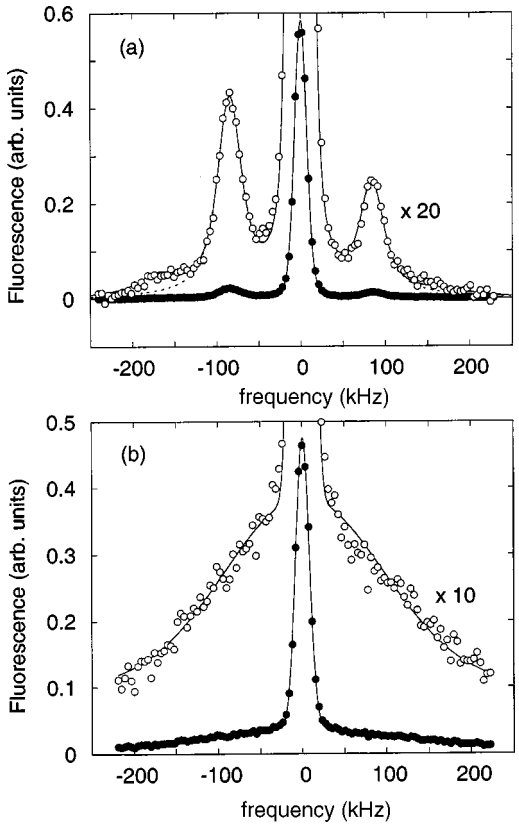

Fig. 9. (a) Fluorescence spectrum in a 1D lin $\perp$ lin optical molasses. Atoms are first captured and cooled in an MOT; then the MOT light beams are switched off, leaving a pair of lin $\perp$ lin beams. Then the measurements are made with $\delta = -4\gamma$ at low intensity. The open symbols are scaled up to emphasize the sidebands by a factor of 20 compared with the original data indicated by the filled symbols. The center peak is due to spontaneous emission of the atoms to the same vibrational state from which they are excited, whereas the sideband on the left (right) is due to spontaneous emission to a vibrational state with one vibrational quantum number lower (higher) (see Fig. 8). The presence of these sidebands is a direct proof of the existence of the band structure. (b) Same as (a) except the 1D molasses is $\sigma^+ - \sigma^-$, which has no spatially dependent light shift and hence no vibrational states (from Ref. 47).

that load atoms directly into a lattice from a Bose–Einstein condensate (BEC), the filling factor can be increased to 100%, and in some cases it may be possible to load more than one atom per lattice site.[51,52]

Because of the transverse nature of light, any mixture of beams with different **k**-vectors necessarily produces a spatially periodic, inhomogeneous light field. The importance of the "egg-crate" array of potential wells arises because the associated atomic light shifts can easily be comparable to the very low average atomic kinetic energy of laser-cooled atoms. A typical example projected against two dimensions is shown in Fig. 10.

In 1993 a very clever scheme was described.[53] It was realized that an n-dimensional lattice could be created by only $n + 1$ traveling waves rather than $2n$. The real benefit of this scheme is that in the case of phase instabilities in the laser beams the interference pattern is shifted only in space, but the interference pattern itself is not changed. Instead of producing optical wells in two dimensions with four beams (two standing waves), Grynberg *et al.*[53] used only three. The **k** vectors of the coplanar beams were separated by $2\pi/3$, and they were all linearly polarized in their common plane (not parallel to one another) The same immunity to vibrations was established for a 3D optical lattice by use of only four beams arranged in a quasi-tetrahedral configuration. The three linearly polarized beams of the 2D arrangement described above were directed out of the plane toward a common vertex, and a fourth circularly polarized beam was added. All four beams were polarized in the same plane. Grynberg *et al.*[53] showed that this configuration produced the desired potential wells in three dimensions.

3. Spectroscopy in 3D Lattices

The NIST group studied atoms loaded into an optical lattice by using Bragg diffraction of laser light from the spatially ordered array.[54] They cut off the laser beams that formed the lattice, and before the atoms had time to move away from their positions, they pulsed on a probe laser beam at the Bragg angle appropriate for one of the sets of lattice planes. The Bragg diffraction not only enhanced the reflection of the probe beam by a factor of 10^5 but, by varying the time between the shutoff of the lattice and turnon of the probe, they could measure the temperature of the atoms in the lattice. The reduction of the amplitude of the Bragg scattered beam with time provided some measure of the diffusion of the atoms away from the lattice sites, much like the Debye–Waller factor in x-ray diffraction.

The group at NIST also developed a new method that superposed a weak probe beam of light directly from the laser upon some of the fluorescent light from the atoms in a 3D optical molasses, and they directed the light from these combined sources onto on a fast photodetector.[55] The resulting beat signal carried information about the Doppler shifts of the atoms in the optical lattices.[47] These Doppler shifts were expected to be in the submegahertz range for atoms with the previously measured 50-μK temperatures. The observed features confirmed the quantum nature of the motion of atoms in the wavelength-size potential wells[15] (see Fig. 9).

4. Quantum Transport in Optical Lattices

In the 1930s Bloch realized that applying a uniform force to a particle in a periodic potential would not accelerate it beyond a certain speed, but instead would result in Bragg reflection when its de Broglie wavelength became equal to the lattice period. Thus an electric field applied to a conductor could not accelerate electrons to a speed faster than that corresponding to the edge of a Brillouin zone, and at longer times the particles would execute oscillatory motion. Ever since then experimentalists have tried to observe these Bloch oscillations in increasingly pure or defect-free crystals.

Atoms moving in optical lattices are ideally suited for such an experiment, as was beautifully demonstrated in 1996.[56] Ben Dahan *et al.* loaded a 1D lattice with atoms from a 3D molasses, further narrowed the velocity distribution, and then, instead of applying a constant force, simply changed the frequency of one of the beams of the 1D lattice with respect to the other in a controlled way, thereby creating an accelerating lattice. Seen from the atoms' reference frame, this was the equivalent of a constant force trying to accelerate them. After a variable time t_a the 1D lattice beams were shut off, and the measured atomic velocity distribution showed beautiful Bloch oscillations as a function of t_a. The centroid of the very narrow velocity distribution was seen to shift in velocity space at a constant rate until it reached $v_r = \hbar k/M$, and then it vanished and reappeared at $-v_r$ as shown in Fig. 11. The shape of the dispersion curve allowed measurement of the effective mass of the atoms bound in the lattice.

4. MULTILEVEL ATOMS

A. Introduction

In the late 1980s it became apparent that the simplified view of optical forces on moving atoms that was based on two-level atoms in a single-frequency light field would not suffice for many phenomena. Although this picture was adequate for beam slowing, optical traps, and lattices, and even provided a primitive description of optical molasses, the consideration of the multilevel structure of atoms was necessary for other phenomena.

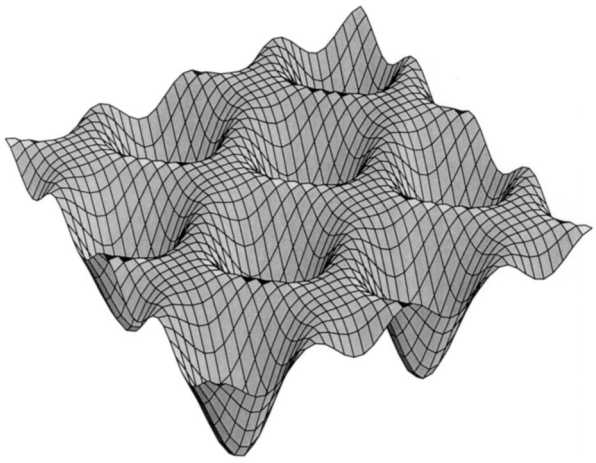

Fig. 10. Egg-crate potential of an optical lattice shown in two dimensions. The potential wells are separated by $\lambda/2$.

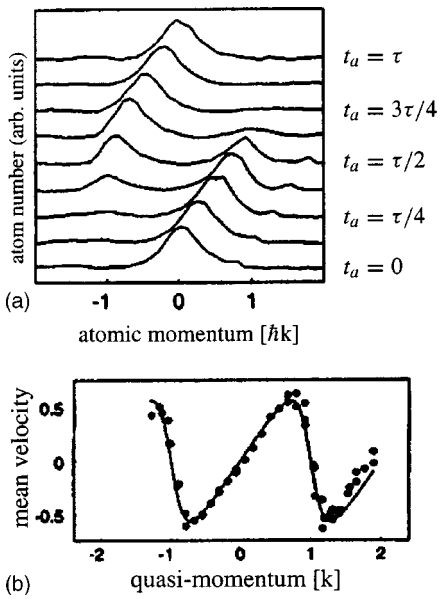

Fig. 11. Plot of the measured velocity distribution versus time in the accelerated 1D lattice. (a) Atoms in a 1D lattice are accelerated for a certain time t_a, and the momentum of the atoms after the acceleration is measured. The atoms accelerate only to the edge of the Brillouin zone, where the velocity is $+v_r$, and then the velocity distribution appears at $-v_r$. (b) Mean velocity of the atoms as a function of the quasi-momentum, i.e., the force times the acceleration time (from Ref. 56).

Perhaps the greatest stimulus for the extension to multilevel atoms came from the measurement of laser-cooled temperatures below the Doppler limit[15] T_D that eventually led to the idea of Sisyphus cooling in polarization gradients. Other phenomena that depended on the internal structure of real atoms included VSCPT, MOTs, various specialized kinds of optical lattices, and many schemes that depended on optical pumping among various atomic sublevels such as magnetically induced laser cooling. Many of these topics are discussed below.

B. Cooling Below the Doppler Limit

1. Introduction

In response to the surprising measurements of temperatures below T_D discussed at the end of subsection 2.B.3, two groups developed a model of laser cooling that could explain the lower temperatures.[57,58] The key feature of this model that distinguishes it from the earlier picture was the inclusion of the multiplicity of sublevels that make up an atomic state (e.g., Zeeman and hfs). The dynamics of optically pumping moving atoms among these sublevels provides the new mechanism for producing the ultralow temperatures.[59]

The dominant feature of these models is the nonadiabatic response of moving atoms to the light field. Atoms at rest in a steady state have ground-state orientations caused by optical pumping processes that distribute the populations over the different ground-state sublevels. In the presence of polarization gradients, these orientations reflect the local light field. In the low-light-intensity regime, the orientation of stationary atoms is completely determined by the ground-state distribution: The optical coherences and the exited-state population follow the ground-state distribution adiabatically.

For atoms moving in a light field that varies in space, optical pumping acts to adjust the atomic orientation to the changing conditions of the light field. In a weak pumping process, the orientation of moving atoms always lags behind the orientation that would exist for stationary atoms. It is this phenomenon of nonadiabatic following that is the essential feature of the new cooling process.

Production of spatially dependent optical pumping processes can be achieved in several different ways. As an example, consider two counterpropagating laser beams that have orthogonal polarizations, as discussed below. The superposition of the two beams results in a light field having a polarization that varies on the wavelength scale along the direction of the laser beams. Laser cooling by such a light field is called polarization gradient cooling. In a 3D optical molasses the transverse wave character of light requires that the light field always have polarization gradients.

2. Linear ⊥ Linear Polarization Gradient Cooling

One of the most instructive models for discussion of sub-Doppler laser cooling was introduced in Ref. 57 and very well described in Ref. 59. If the polarizations of two counterpropagating laser beams are identical, the two beams interfere and produce a standing wave. When the two beams have orthogonal linear polarizations (same frequency ω_ℓ) with their $\hat{\mathcal{E}}$ vectors perpendicular (e.g., $\hat{x}$ and $\hat{y}$), the configuration is called lin ⊥ lin or lin-perp-lin. Then the total field is the sum of the two counterpropagating beams given by

$$\begin{aligned}\boldsymbol{\mathcal{E}} &= \mathcal{E}_0\hat{x}\cos(\omega_\ell t - kz) + \mathcal{E}_0\hat{y}\cos(\omega_\ell t + kz)\\ &= \mathcal{E}_0[(\hat{x}+\hat{y})\cos\omega_\ell t\cos kz + (\hat{x}-\hat{y})\sin\omega_\ell t\sin kz].\end{aligned} \tag{14}$$

At the origin, where $z = 0$, this becomes

$$\boldsymbol{\mathcal{E}} = \mathcal{E}_0(\hat{x}+\hat{y})\cos\omega_\ell t, \tag{15}$$

which corresponds to linearly polarized light at an angle $+\pi/4$ to the x axis. The amplitude of this field is $\sqrt{2}\mathcal{E}_0$. Similarly, for $z = \lambda/4$, where $kz = \pi/2$, the field is also linearly polarized but at an angle $-\pi/4$ to the x axis.

Between these two points, at $z = \lambda/8$, where $kz = \pi/4$, the total field is

$$\boldsymbol{\mathcal{E}} = \mathcal{E}_0[\hat{x}\sin(\omega_\ell t + \pi/4) - \hat{y}\cos(\omega_\ell t + \pi/4)]. \tag{16}$$

Since the $\hat{x}$ and $\hat{y}$ components have sine and cosine temporal dependence, they are $\pi/2$ out of phase, and so Eq. (16) represents circularly polarized light rotating about the z axis in the negative sense. Similarly, at $z = 3\lambda/8$, where $kz = 3\pi/4$, the polarization is circular but in the positive sense. Thus in this lin ⊥ lin scheme the polarization cycles from linear to circular to orthogonal linear to opposite circular in the space of only half a wavelength of light, as shown in Fig. 12. It truly has a very strong polarization gradient.

Since the coupling of the different states of multilevel atoms to the light field depends on its polarization, atoms moving in a polarization gradient will be coupled differ-

ently at different positions, and this will have important consequences for laser cooling. For the $J_g = 1/2 \rightarrow J_e = 3/2$ transition (one of the simplest transitions that show sub-Doppler cooling[60]), the optical pumping process in purely σ^+ light drives the ground-state population to the $M_g = +1/2$ sublevel. This optical pumping occurs because absorption always produces $\Delta M = +1$ transitions, whereas the subsequent spontaneous emission produces $\Delta M = \pm 1, 0$. Thus the average $\Delta M \geqslant 0$ for each scattering event. For σ^- light the population is pumped toward the $M_g = -1/2$ sublevel. Thus atoms traveling through only a half-wavelength in the light field need to readjust their population completely from $M_g = +1/2$ to $M_g = -1/2$ and back again.

The interaction between nearly resonant light and atoms not only drives transitions between atomic energy levels but also shifts their energies. This light shift of the atomic energy levels plays a crucial role in this scheme of sub-Doppler cooling, and the changing polarization has a strong influence on the light shifts. In the low-intensity limit of two laser beams, each of intensity $s_0 I_s$, the light shifts ΔE_g of the ground magnetic substates are given by a slight variation of Eq. (3) that accounts for the multilevel structure of the atoms. We write

$$\Delta E_g = \frac{\hbar \delta s_0 C_{ge}^2/2}{1 + (2\delta/\gamma)^2}, \tag{17}$$

where C_{ge} is the Clebsch–Gordan coefficient that describes the coupling between the particular levels of the atom and the light field.

In the present case of orthogonal linear polarizations and $J = 1/2 \rightarrow 3/2$, the light shift for the magnetic substate $M_g = 1/2$ is three times larger than that of the $M_g = -1/2$ substate when the light field is completely σ^+. On the other hand, when an atom moves to a place where the light field is σ^-, the shift of $M_g = -1/2$ is three times larger. So in this case the optical pumping discussed above causes there to be a larger population in the state with the larger light shift. This is generally true for any transition J_g to $J_e = J_g + 1$. A schematic diagram showing the populations and light shifts for this particular case of negative detuning is shown in Fig. 13.

3. Origin of the Damping Force

To discuss the origin of the cooling process in this polarization gradient scheme, consider atoms with a velocity v at a position where the light is σ^+ polarized, as shown at the lower left of Fig. 13. The light optically pumps such atoms to the strongly negative light-shifted $M_g = +1/2$ state. In moving through the light field, atoms must increase their potential energy (climb a hill) because the polarization of the light is changing and the state $M_g = 1/2$ becomes less strongly coupled to the light field. After traveling a distance $\lambda/4$, atoms arrive at a position where the light field is σ^- polarized and are optically pumped to $M_g = -1/2$, which is now lower than the $M_g = 1/2$ state. Again the moving atoms are at the bottom of a hill and start to climb. In climbing the hills, the kinetic energy is converted to potential energy, and in the optical pumping process the potential energy is radiated away because the spontaneous emission is at a higher frequency than the absorption (see Fig. 13). Thus atoms seem to be always climbing hills and losing energy in the process. This process brings to mind a Greek myth and is thus called Sisyphus laser cooling.

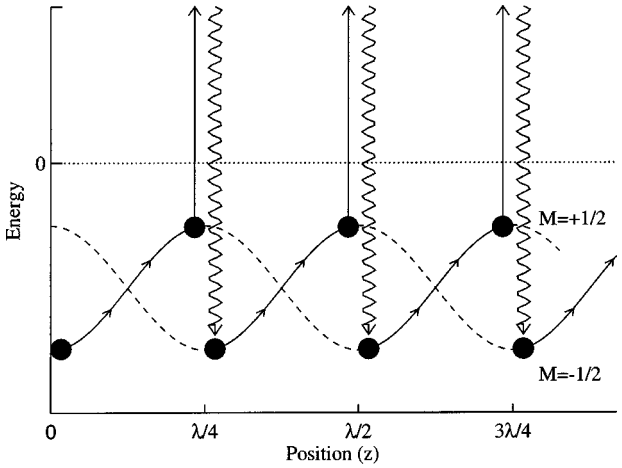

Fig. 13. Spatial dependence of the light shifts of the ground-state sublevels of the $J = 1/2 \Leftrightarrow 3/2$ transition for the case of the lin $\perp$ lin polarization configuration. The arrows show the path followed by atoms being cooled in this arrangement. Atoms starting at $z = 0$ in the $M_g = +1/2$ sublevel must climb the potential hill as they approach the $z = \lambda/4$ point where the light becomes σ^- polarized, and there they are optically pumped to the $M_g = -1/2$ sublevel. Then they must begin climbing another hill toward the $z = \lambda/2$ point, where the light is σ^+ polarized and they are optically pumped back to the $M_g = +1/2$ sublevel. The process repeats until the atomic kinetic energy is too small to climb the next hill. Each optical pumping event results in absorption of light at a lower frequency than emission, thus dissipating energy to the radiation field.

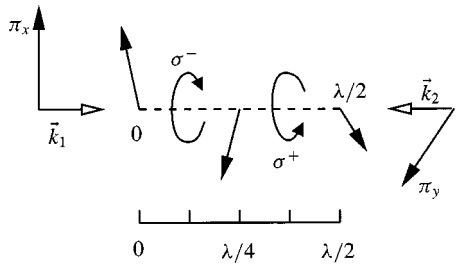

Fig. 12. Polarization gradient field for the lin $\perp$ lin configuration.

The cooling process described above is effective over a limited range of atomic velocities. The force is maximum for atoms that undergo one optical pumping process while traveling a distance $\lambda/4$. Slower atoms will not reach the hilltop before the pumping process occurs, and faster atoms will already be descending the hill before being pumped toward the other sublevel. In both cases the energy loss is smaller, and therefore the cooling process less efficient. Nevertheless, the damping constant β for this process is much larger than for Doppler cooling, and therefore the final steady-state temperature is lower.[57,59]

In the experiments of Ref. 61 the temperature was measured in a 3D molasses under various configurations of the polarization. Temperatures were measured by a ballistic technique, where the flight time of the released atoms was measured as they fell through a probe a few centimeters below the molasses region. The lowest tem-

perature obtained is 3 μK, which is a factor 40 below the Doppler temperature and a factor 15 above the recoil temperature of Cs.

4. Magnetically Induced Laser Cooling

Although the first models that described sub-Doppler cooling relied on the polarization gradient of the light field as above, it was soon discovered that a light field of constant polarization in combination with a magnetic field could also produce sub-Doppler cooling.[62] In this process the atoms are cooled in a standing wave of circularly polarized light.

There is a simple model using the $J_g = 1/2$ to $J_e = 3/2$ transition to describe this phenomenon.[63] In the absence of a magnetic field, the σ^+ light field drives the population to the $M_g = +1/2$ sublevel. Since the $M_g = +1/2$ sublevel is more strongly coupled to the light field than is $M_g = -1/2$, the light shift of this state is larger. Thus atoms traveling through this standing wave will descend and climb the same potential hills corresponding to $M_g = 1/2$ and will experience no average force.

The situation changes if a small transverse magnetic field is applied. Optical pumping processes determine the atomic states in the antinodes of the standing wave light field where the light is strong. But in the nodes, where the intensity of the light field is zero, the small transverse magnetic field precesses the population from $M_g = 1/2$ toward $M_g = -1/2$. Atoms that leave the nodes with $M_g = -1/2$ are returned to $M_g = +1/2$ in the antinodes by optical pumping in the σ^+ light.

This cooling process is depicted in Fig. 14 for negative detuning $\delta < 0$. Potential energy is radiated away in the optical pumping process as before, and kinetic energy is converted to potential energy when the atoms climb the hills again into the nodes. The whole process is repeated when the atoms travel through the next node of the light field. Again the cooling process is caused by a Sisyphus effect, similar to the case of lin $\perp$ lin. Since this damping force is absent without the magnetic field, it is called magnetically induced laser cooling (MILC).

Efficient cooling by MILC depends critically on the relation between the Zeeman precession frequency ω_Z and the optical pumping rate γ_p in the antinodes. It is clearly necessary that $\gamma_p \gg \omega_Z$ in the antinodes where the light is strong. But, as in any cooling process that depends on nonadiabatic processes, there is a limited velocity range where the force is effective. For efficient cooling by MILC, the velocity cannot be too small compared with ω_Z/k or atoms will undergo many precession cycles near the nodes, and no effective cooling will result. On the other hand, if the velocity is large compared with γ_p/k, then atoms will pass through the antinodes in a time too short to be optically pumped to $M_g = +1/2$, and no cooling will result either. Thus, in addition to the requirement $\delta < 0$, there are two other conditions on the experimental parameters that can be combined to give

$$\omega_Z < kv < \gamma_p . \tag{18}$$

Sub-Doppler cooling has been observed for MILC in Rb atoms cooled on the $\lambda = 780$ nm transition in one dimension.[63] The width of the velocity distribution near $v = 0$ is as low as 2 cm/s, much lower than the 1D Doppler limit $v_D = \sqrt{7\hbar\gamma/20M} \approx 10$ cm/s for Rb.

5. Limits of Laser Cooling

The extension of the kind of thinking of temperature in the case of Doppler cooling to the case of the sub-Doppler processes must be done with some care, because a naïve application of the consequences of the Fokker–Planck equation would lead to an arbitrarily low final temperature. In the derivation of the Fokker–Planck equation it is explicitly assumed that each scattering event changes the atomic momentum p by an amount that is a small fraction of p, and this clearly fails when the velocity is reduced to the region of $v_r \equiv \hbar k/M$.

This limitation of the minimum steady-state value of the average kinetic energy to a few times $2E_r \equiv k_B T_r = Mv_r^2$ is intuitively comforting for two reasons. First, one might expect that the last spontaneous emission in a cooling process would leave atoms with a residual momentum of the order of $\hbar k$, since there is no control over its direction. Thus the randomness associated with this would put a lower limit on such cooling of $v_{\min} \sim v_r$. Second, the polarization gradient cooling mechanism described above requires that atoms be localizable within the scale of $\sim\lambda/2\pi$ in order to be subject to only a single polarization in the spatially inhomogeneous light field. The uncertainty principle then requires that these atoms have a momentum spread of at least $\hbar k$.

The recoil limit discussed here has been surpassed by evaporative cooling of trapped atoms[64] and two different

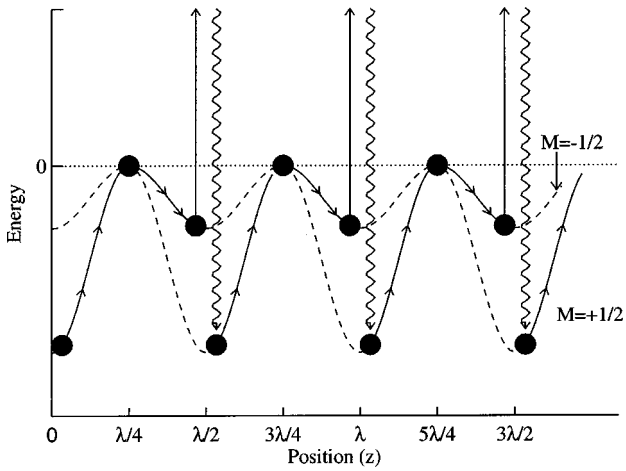

Fig. 14. Spatial dependence of the light shifts of the ground-state sublevels of the $J = 1/2 \Leftrightarrow 3/2$ transition for the case of a purely σ^+ standing wave that has no polarization gradient and is appropriate for magnetically induced laser cooling. The arrows show the path followed by atoms being cooled in this arrangement. Atoms starting at $z = 0$ in the strongly light-shifted $M_g = +1/2$ sublevel must climb the potential hill as they approach the node at $z = \lambda/4$. There they undergo Zeeman mixing in the absence of any light and may emerge in the $M_g = -1/2$ sublevel. They will then gain less energy as they approach the antinode at $z = \lambda/2$ than they lost climbing into the node. Then they are optically pumped back to the $M_g = +1/2$ sublevel in the strong light of the antinode, and the process repeats until the atomic kinetic energy is too small to climb the next hill. Each optical pumping event results in absorption of light at a lower frequency than emission, thus dissipating energy to the radiation field.

optical cooling methods, neither of which can be based in simple notions. One of these uses optical pumping into a velocity-selective dark state and is described in Subsection 3.A above. The other one uses carefully chosen, counterpropagating laser pulses to induce velocity-selective Raman transitions and is called Raman cooling.[65]

C. Magneto-Optical Traps

1. Introduction

The most widely used trap for neutral atoms is a hybrid, employing both optical and magnetic fields, to make a MOT, first demonstrated in 1987.[66] The operation of a MOT depends on both inhomogeneous magnetic fields and radiative selection rules to exploit both optical pumping and the strong radiative force.[66,67] The radiative interaction provides cooling that helps in loading the trap, and enables very easy operation. The MOT is a very robust trap that does not depend on precise balancing of the counterpropagating laser beams or on a very high degree of polarization. The magnetic field gradients are modest and can readily be achieved with simple, air-cooled coils. The trap is easy to construct because it can be operated with a room-temperature cell where alkali atoms are captured from the vapor. Furthermore, low-cost diode lasers can be used to produce the light appropriate for many atoms, so the MOT has become one of the least expensive ways to make atomic samples with temperatures below 1 mK.

Trapping in a MOT works by optical pumping of slowly moving atoms in a linearly inhomogeneous magnetic field $B = B(z) \equiv Az$, such as that formed by a magnetic quadrupole field. Atomic transitions with the simple scheme of $J_g = 0 \rightarrow J_e = 1$ have three Zeeman components in a magnetic field, excited by each of three polarizations, whose frequencies tune with field (and therefore with position) as shown in Fig. 15 for one dimension. Two counterpropagating laser beams of opposite circular polarization, each detuned below the zero-field atomic resonance by δ, are incident as shown.

Because of the Zeeman shift, the excited state $M_e = +1$ is shifted up for $B > 0$, whereas the state with $M_e = -1$ is shifted down. At position z' in Fig. 15 the magnetic field therefore tunes the $\Delta M = -1$ transition closer to resonance and the $\Delta M = +1$ transition further out of resonance. If the polarization of the laser beam incident from the right is chosen to be σ^- and correspondingly σ^+ for the other beam, then more light is scattered from the σ^- beam than from the σ^+ beam. Thus the atoms are driven toward the center of the trap where the magnetic field is zero. On the other side of the center of the trap, the roles of the $M_e = \pm 1$ states are reversed, and now more light is scattered from the σ^+ beam, again driving the atoms towards the center.

The situation is analogous to the velocity damping in an optical molasses from the Doppler effect as discussed in Subsection 2.B, but here the effect operates in position space, whereas for molasses it operates in velocity space. Since the laser light is detuned below the atomic resonance in both cases, compression and cooling of the atoms is obtained simultaneously in a MOT.

So far the discussion has been limited to the motion of atoms in one dimension. However, the MOT scheme can easily be extended to three dimensions by using six instead of two laser beams. Furthermore, even though very few atomic species have transitions as simple as $J_g = 0 \rightarrow J_e = 1$, the scheme works for any $J_g \rightarrow J_e = J_g + 1$ transition. Atoms that scatter mainly from the σ^+ laser beam will be optically pumped toward the $M_g = +J_g$ substate, which forms a closed system with the $M_e = +J_e$ substate.

2. Cooling and Compressing Atoms in a MOT

For a description of the motion of the atoms in a MOT, consider the radiative force in the low-intensity limit [see Eqs. (1) and (2)]. The total force on the atoms is given by $\mathbf{F} = \mathbf{F}_+ + \mathbf{F}_-$, where $\mathbf{F}_\pm$ can be found from Eqs. (1) and (2), and the detuning $\delta_\pm$ for each laser beam is given by $\delta_\pm = \delta \mp \mathbf{k} \cdot \mathbf{v} \pm \mu' B/\hbar$. Here $\mu' \equiv (g_e M_e - g_g M_g)\mu_B$ is the effective magnetic moment for the transition used. Note that the Doppler shift $\omega_D \equiv -\mathbf{k} \cdot \mathbf{v}$ and the Zeeman shift $\omega_Z = \mu' B/\hbar$ both have opposite signs for opposite beams.

When both the Doppler and Zeeman shifts are small compared with the detuning δ, the denominator of the force can be expanded as for relation (5) and the result becomes

$$\mathbf{F} = -\beta \mathbf{v} - \kappa \mathbf{r}, \tag{19}$$

where the damping coefficient β is defined in relation (5). The spring constant κ arises from the similar dependence of $\mathbf{F}$ on the Doppler and Zeeman shifts and is given by $\kappa = \mu' A \beta/\hbar k$.

The force of Eq. (19) leads to damped harmonic motion of the atoms, where the damping rate is given by $\Gamma_{\mathrm{MOT}} = \beta/M$ and the oscillation frequency $\omega_{\mathrm{MOT}} = \sqrt{\kappa/M}$. For magnetic field gradients $A \approx 10$ G/cm, the oscillation frequency is typically a few kilohertz, and this is much smaller than the damping rate that is typically a few hundred kilohertz. Thus the motion is overdamped, with a

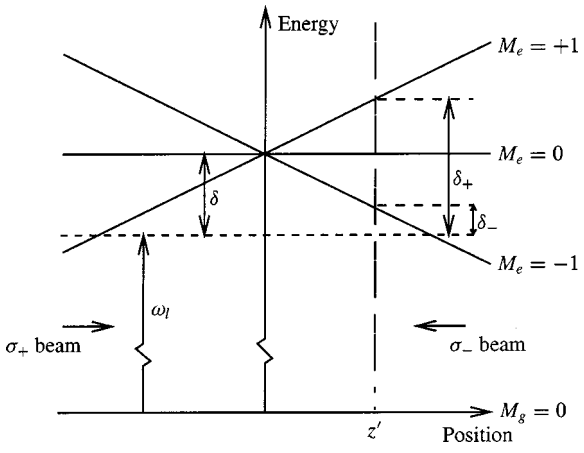

Fig. 15. Arrangement for a MOT in one dimension. The horizontal dashed line represents the laser frequency seen by an atom at rest in the center of the trap. Because of the Zeeman shifts of the atomic transition frequencies in the inhomogeneous magnetic field, atoms at $z = z'$ are closer to resonance with the σ^- laser beam than with the σ^+ beam and are therefore driven toward the center of the trap.

characteristic restoring time to the center of the trap of $2\Gamma_{\mathrm{MOT}}/\omega_{\mathrm{MOT}}^2 \approx$ several milliseconds for typical values of the detuning and intensity of the lasers.

3. Capturing Atoms in a MOT

Although the approximations that lead to Eq. (19) for the force hold for slow atoms near the origin, they do not apply for the capture of fast atoms far from the origin. In the capture process the Doppler and Zeeman shifts are no longer small compared with the detuning, so the effects of the position and velocity can no longer be disentangled. However, the full expression for the force still applies, and the trajectories of the atoms can be calculated by numerical integration of the equation of motion.[68]

The capture velocity of a MOT is serendipitously enhanced because atoms traveling across it experience a decreasing magnetic field just as in the beam deceleration described in Subsection 2.A. This enables resonance over an extended distance and velocity range because the changing Doppler shift of decelerating atoms can be compensated by the changing Zeeman shift as atoms move in the inhomogeneous magnetic field. Of course, it will work this way only if the field gradient A does not demand an acceleration larger than the maximum acceleration a_{max}. Thus atoms are subject to the optical force over a distance that can be as long as the trap size, and they can therefore be slowed considerably.

The very large velocity capture range v_{cap} of a MOT can be estimated by using $F_{\mathrm{max}} = \hbar k\gamma/2$ and choosing a maximum size of a few centimeters for the beam diameters. Thus the energy change can be as large as a few kelvin, corresponding to $v_{\mathrm{cap}} \sim 100$ m/s (Ref. 67). The number of atoms in a vapor with velocities below v_{cap} in the Boltzmann distribution scales as v_{cap}^4, and there are enough slow atoms to fall within the large MOT capture range even at room temperature, because a few kelvin includes 10^{-4} of the atoms.

4. Variations on the MOT Technique

Because of the wide range of applications of this most versatile kind of atom trap, a number of careful studies of its properties have been made,[67,69–75] and several variations have been developed. One of these is designed to overcome the density limits achievable in a MOT. In the simplest picture, loading additional atoms into a MOT produces a higher atomic density because the size of the trapped sample is fixed. However, the density cannot increase without limit as more atoms are added. The atomic density is limited to $\sim 10^{11}$ cm^{-3} because the fluorescent light emitted by some trapped atoms is absorbed by others.

One way to overcome this limit is to have much less light in the center of the MOT than at the sides. Simply lowering the laser power is not effective in reducing the fluorescence because it will also reduce the capture rate and trap depth. But those advantageous properties can be preserved while reducing fluorescence from atoms at the center if the light intensity is low only in the center.

The repumping process for the alkali atoms provides an ideal way of implementing this idea.[76] If the repumping light is tailored to have zero intensity at the center, then atoms trapped near the center of the MOT are optically pumped into the wrong hfs state and stop fluorescing. They drift freely in the dark at low speed through the center of the MOT until they emerge on the other side into the region where light of both frequencies is present and they begin absorbing again. Then they feel the trapping force and are driven back into the dark center of the trap. Such a MOT has been operated at MIT[76] with densities close to 10^{12} cm^{-3}, and the limitations are now from collisions in the ground state rather than from multiple light scattering and excited-state collisions.

5. POLYCHROMATIC LIGHT

A. Introduction

In the introductory Sections 1 and 2 of this paper, the ideas of laser cooling are discussed in terms of two-level atoms moving in a monochromatic laser beam. Section 4 shows that this simple view is inadequate and that the multiple level structure of atoms is necessary to explain some experiments. The extension from two-level to multilevel atoms gives an unexpected richness to the topic of atomic motion in optical fields. It seems natural to expect that a comparable multitude of new phenomena is to be found for the motion of two level atoms in multifrequency fields, but this subject has not received as much attention.

In the Doppler cooling process of two-level atoms described in Subsection 2.B, it is the radiative force that produces *both* the slowing force *and* the dissipation necessary for cooling. The force arises from the incoherent sequence of absorption followed by spontaneous emission. Thus it is limited to $F \leqslant \hbar k\gamma/2$.

By contrast, in most cases of laser cooling in multilevel atoms, such as Sisyphus cooling in a polarization gradient as discussed in Subsection 4.B, it is the dipole force that works on the atoms. This force is usually present in multiple beams of monochromatic light such as standing waves. Since this force results from the rapid coherent sequence of absorption followed by stimulated emission, it does not suffer from such limits.

Although this force can be very strong, its sign alternates in space on the wavelength scale, and thus its spatial average vanishes. Moreover, this force is completely conservative so its cooling aspect, or velocity dependence, must arise from the relatively infrequent spontaneous emission events, and so such sub-Doppler cooling forces are similarly limited to a maximum of $F_{\mathrm{rad}} = \hbar k\gamma/2$. Thus not only is the cooling aspect of the dipole force limited in strength, but also the spatial average of the strong conservative component vanishes.

In 1997 there was a dramatic demonstration of the use of a bichromatic field with two beams of equal intensities and detunings that provided both a strong force and wide velocity range.[77] Using only modest laser power, Söding *et al.* demonstrated that this bichromatic force could decelerate a thermal beam of Cs to $\sim$20 m/s in just a few centimeters with no Doppler compensation.

Unlike the limited velocity range of the rectified dipole force,[78,79] the bichromatic force has both a very large velocity range and magnitude. Since the force covers a much larger range of velocities, Doppler compensation, such as using a multikilowatt Zeeman tuning magnet, is

rendered unnecessary for slowing a thermal beam. Thus it is a valuable method for fast, short-distance deceleration of thermal atoms that minimizes atom loss, thereby making it a most useful and important tool in the production of cold, dense atomic samples for traps, lithography, and other purposes.

Another way to make polychromatic light is to frequency modulate a single beam. In this case the parameters available are the rate of frequency modulation ω_m and the strength of the modulation, characterized by a dimensionless parameter β. For weak modulation the light can be considered a carrier with sidebands, but that topic is not pursued in this paper.[80] For stronger modulation the dynamics of the atomic response changes, and the adiabatic rapid passage (ARP) picture is appropriate (see Subsection 5.C below).

B. Bichromatic Force

1. Basic Ideas

The bichromatic force has a velocity range very much larger than the usual velocity range γ/k for slowing by radiative forces, and it also has a strong velocity dependence at its range boundaries so that it can cool.[77] Naturally this (dissipative) velocity dependence originates from the occasional spontaneous emission events at a rate determined by γ, but the magnitude of the force is not limited by this rate. Using two frequencies provides extra degrees of freedom for the light field, and these have been exploited to make forces substantially larger than the radiative force and cover a wider velocity range than the rectified force or Sisyphus cooling.[80–84]

Suppose an atom is exposed to resonant light of Rabi frequency Ω for a time t_π that satisfies $\Omega t_\pi = \pi$. Then the atom is driven from the ground to excited state (or vice versa). Such a "π pulse" provides an intuitive model for the bichromatic force. Consider atomic motion along the axis of counterpropagating bichromatic light beams. Each beam contains the same two frequencies, and they are detuned from atomic resonance by $\pm\delta$ (difference frequency $= 2\delta$). Each beam can be described as an amplitude-modulated single carrier frequency at the atomic resonance frequency ω_a having modulation period π/δ, and δ is chosen such that $\pi/\delta \ll \tau$ or $\delta \gg \gamma$. The equal intensities of each beam are chosen so that the envelope of one pulse of the beats satisfies the condition of a π pulse for the atoms: Ground-state atoms are coherently driven to the excited state and vice versa. This condition is $\Omega = \pi\delta/4$, where $\Omega \equiv \gamma\sqrt{I/2I_s}$ is the Rabi frequency associated with each frequency component of each beam.

Atoms in this light field are subject to these π pulses alternately from one beam direction and then from the other, so the force on them can become very large. This is because the first π pulse causes excitation along with momentum transfer in one direction, and the second counterpropagating π pulse causes stimulated emission, producing a momentum transfer *along the same direction as the first pulse*.

Thus atoms are coherently driven between the ground and the excited states, and momentum is monotonically exchanged with the light field. The magnitude of the momentum transfer in each cycle is $2\hbar k$, and the repetition rate of these controlled processes is δ/π, so that the optimum total force is of the order of $2\hbar k\,\delta/\pi$. This is *very* much larger than the usual maximum radiative force $\hbar k\,\gamma/2$, principally because it is a coherently controlled rapid momentum exchange whose rate is limited only by laser power through the π-pulse condition. The bichromatic force is *not* subject to saturation.

The mechanism described above requires two additional features to be applicable to atomic beam slowing: (1) There must be some directional asymmetry because the excitation pulse could come from either direction, and thus the force could point either way, and (2) it must be velocity dependent so that it can compress the phase-space volume of the atomic sample.

The first condition is satisfied by a careful choice of the relative intervals between the counterpropagating pulses of light (i.e., the relative phase of the modulation) and exploitation of the random nature of spontaneous emission. If the pulses are evenly spaced, spontaneous emission spoils the cycle described above, since an excited atom can spontaneously decay to the ground state so that the next pulse causes absorption rather than stimulated emission. Thus each spontaneous emission produces a reversal in the direction of the force, resulting in zero average force.

However, if the pulses are timed unevenly so that they come in closely spaced pairs, one from each direction, their asymmetry indeed produces a preferred direction. When the first pulse of each closely spaced pair produces excitation, the atom spends less time in the excited state before stimulated emission by the second pulse, resulting in a lower probability for spontaneous emission that would reverse the force. Just the opposite situation prevails for an atom excited by the second pulse of a pair, because spontaneous emission is more likely to occur in the longer interval than in the shorter one when $\tau \gg \pi/\delta$. While it is still possible for an atom to get into a cycle that will produce a force in either direction, atoms that get out of phase with the preferred order by suffering spontaneous emission during the short interval are more likely to undergo correction than to remain out of phase, so there will be more events that produce a force in the direction of travel of the leading pulse. This model was experimentally realized in Ref. 85 on Cs by use of picosecond π pulses from a pulsed laser.

The optimum phase difference between the beats in the counterpropagating beams has been found by numerical calculations to be $\cong\pi/4$, so that atoms typically experience a force in the wrong direction for 25% of their time. Then the same 25% is needed to negate this undesired force, leaving 50% of the time for the desired force. Thus the average force is $\hbar k\,\delta/\pi$, half the optimum estimated above, and this is also borne out by the numerical calculations of Refs. 77, 86, and 87.

The second condition is that the force be velocity dependent in order to cool. Understanding how this arises requires simultaneous consideration of both the light shift *and* the Doppler shift, and the simplified picture of π pulses given above is insufficient. Instead, a dressed-state description of atoms moving in a bichromatic, time-dependent field is required. This has not yet been pro-

vided, and so numerical calculations of the bichromatic force are still required.

2. Experimental Results

Numerical calculations of the bichromatic force using the optical Bloch equations (OBE) have been done for comparison with experiments. The program written by the authors of Ref. 77 works by integrating the OBE for a short time to get past the transients associated with initial conditions, and then calculating the optical force[1] from $F = -\mathrm{tr}(\rho\nabla\mathcal{H})$. The velocity dependence is implemented by Doppler shifting the two frequencies of the beam traveling in one direction up by kv and those from the other direction down by kv.

Figure 16 shows a typical example of the output. For $\delta = 20\gamma$ the magnitude of the force as given by the model above is expected to be $F = \hbar k\delta/\pi = (2\delta/\pi\gamma)F_{\mathrm{rad}} \approx 13F_{\mathrm{rad}}$, and here the average value is about $10\,F_{\mathrm{rad}}$, not very different. Also, the π-pulse condition for the varying envelope of the beat pattern from the two frequencies gives $\Omega = \pi\delta/4$, a value considerably smaller than the $\Omega = 22\gamma$ shown here. Thus these simple models begin to fail when quantitative evaluations are made.

Nevertheless, the velocity range of the force in Fig. 16 is $\approx\delta/k$, and its magnitude corresponds fairly well with the model. The sharp spikes that are ubiquitous in the graph are not artifacts or noise, but correspond to multiphoton effects closely related to Dopplerons.[88] They occur at velocities given by $m\delta/nk$, where m and m are small integers.

There are small features at $v = \pm\delta/k = \pm 20\gamma/k$ in Fig. 16. These occur at the velocity where the upward Doppler shift of $\omega_a - \delta$ and the downward Doppler shift of $\omega_a + \delta$ bring both of these frequencies to atomic resonance, and they correspond to the ordinary Doppler force. Note that their magnitude is confined to less than F_{rad} and their velocity range to a small fraction of γ/k.

The bichromatic force has been used to slow a He* beam (see Ref. 89). The He* source produced a beam with velocity $\approx$1000 m/s $\approx 550\ \gamma/k$ as shown by the dashed curve in Fig. 17. Thus a significant beam deceleration requires a bichromatic force having a range of the order of a few hundred times γ/k.

The measurements used $\delta = 184\gamma = 300$ MHz, so that the range of the bichromatic force is $\approx\delta/k = 184\gamma/k \approx 350$ m/s, and the slowing measurements shown in Fig. 17 demonstrate this velocity range. Moreover, the interaction length was limited by the geometry of the beam overlaps to <5 cm, which is a significant reduction in slowing length compared with slowing with F_{rad}.

The $\approx$100 m/s width of the peak of slowed atoms in the velocity distributions indicates significant cooling in addition to the bichromatic slowing. The factor of three reduction in the velocity spread of the slowed atoms from the initial velocity spread of 300 m/s corresponds to an order of magnitude in temperature reduction.

While short-distance deceleration is applicable for He* trapping experiments, acceleration of the He* beam is also desirable. The direction of the bichromatic force is easily reversed by changing the phase from $\phi = \pi/2$ to $-\pi/2$, and velocity distributions showing acceleration to 1150 m/s have also been observed. The ability to switch the sign of the bichromatic force by controlling the relative phase of the counterpropagating bichromatic fields is a signature effect of the bichromatic force.

C. Adiabatic Rapid Passage Force

The use of π pulses is not the only way to reverse coherently the ground and excited state populations of two-level atoms and thereby mediate controlled momentum exchange. Another way uses the well-known frequency-sweep technique called adiabatic rapid passage (ARP) to invert the population with nearly 100% efficiency.[90–92] ARP is a far more robust method than π pulses because it is not sensitive to variations of the interaction time or the intensity as is the π-pulse method. Changes in the start and end point of the sweep are easily tolerated with little consequence as long as certain conditions on the parameters are satisfied. Thus it seems very attractive to implement this method as a tool for coherently controlled exchange of momentum between atoms and a light field.

A simple model calculation of the magnitude of the ARP-mediated force begins by considering that the momentum transfer in one half-cycle π/ω_m of the frequency-modulated light is $2\hbar k$. First, a frequency-swept laser beam from one direction excites the atoms and transfers

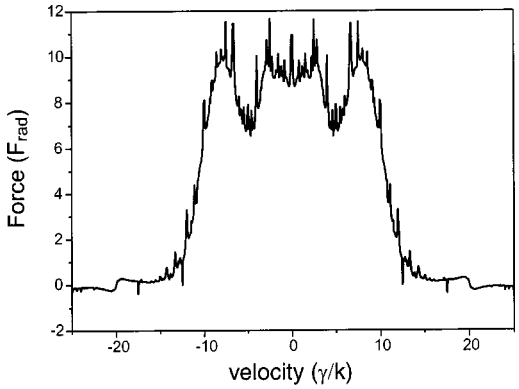

Fig. 16. Bichromatic force on moving atoms in two standing waves of frequencies $\omega_a \pm \delta$, where $\delta = 20\gamma$, plotted in units of $F_{\mathrm{rad}} = \hbar k\gamma/2$. The Rabi frequency for each component of each standing wave was $\Omega = 22\gamma$, and the spatial phase shift between the two standing waves was $\phi = \pi/2$.

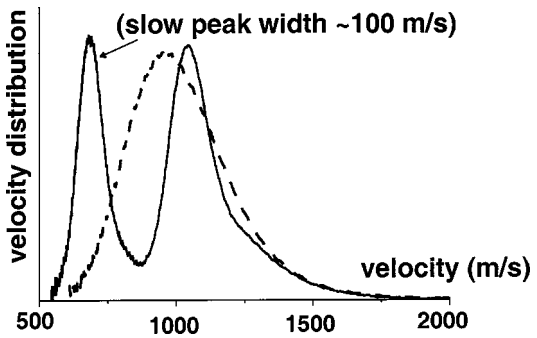

Fig. 17. He* atoms were produced in a LN_2-cooled, dc discharge source with a longitudinal velocity distribution shown by a dashed curve. For these data the detuning $\delta = 184\ \gamma$, $\Omega = 225\ \gamma$, and $\chi = \pi/2$, appropriate for slowing. The laser and atomic beams intersect at a few tens of milliradians, and their diameters determine the interaction length to be a few centimeters.

$\hbar k$, and then another beam from the opposite direction whose sweep is delayed drives them back to the ground state and also transfers $\hbar k$. Since the time for this is π/ω_m, the force is $F_{ARP} \sim 2\hbar k/(\pi/\omega_m) = 2\hbar k\,\omega_m/\pi$.

ARP is particularly well described by use of an artificial Bloch vector $\mathbf{R}$ whose components are determined by the complex coefficients of the superposition of atomic ground and excited states caused by interaction between a two-level atom and the laser light.[93,94] The Schrödinger equation is equivalent to a form where the time dependence of these coefficients satisfies $d\mathbf{R}/dt = \mathbf{\Omega}' \times \mathbf{R}$, where $\mathbf{\Omega}'$ is a torque vector whose two horizontal components are the real and the imaginary parts of the atomic Rabi frequency Ω in the laser field, and the vertical component is the detuning from atomic resonance δ. Thus $|\mathbf{\Omega}'| = \sqrt{|\Omega|^2 + \delta^2}$. (Usually Ω can be chosen to be real.)

This geometric view of the Schrödinger equation allows a particularly graphic interpretation of ARP (see Fig. 18). At the beginning of the frequency sweep, where the initial detuning δ_0 is much larger than the Rabi frequency Ω, $\mathbf{R}$ executes small, rapid orbits near the south pole (atom in the ground state), and the axis of these orbits slowly drifts up toward the equator as δ approaches zero. The sweep continues toward the opposite detuning, so that near the end of the sweep, where again $\delta \gg \Omega$, $\mathbf{R}$ executes small rapid, orbits near the north pole and is finally left at the north pole (the atom is in the excited state). The direction of the frequency sweep, namely the sign of $\dot{\delta}$, is of no consequence as long as $\mathbf{\Omega}'$ is essentially polar at the ends of the sweep.

The electric field $\boldsymbol{\mathcal{E}}_i(z, t)$ of the frequency-modulated plane waves traveling in the $\pm$ directions can be written as

$$\boldsymbol{\mathcal{E}}_{\pm}(z, t) = \mathcal{E}_0 \hat{\varepsilon} \cos[\omega_c t \mp kz + \beta \sin(\omega_m t \pm \chi/2)], \quad (20)$$

where $\hat{\varepsilon}$ is the unit polarization vector and $\mathcal{E}_0$ is the time-independent amplitude of the waves. The waves have equal modulation amplitude $\beta = \delta_0/\omega_m$, where δ_0 is the range of the frequency sweep. The only difference in modulation properties are phase differences χ of each wave. The familiar steady-state spectrum of frequency-modulated light is usually viewed as a carrier with sidebands, but it doesn't seem appropriate for ARP. However, the instantaneous frequency is the time derivative of the phase of $\boldsymbol{\mathcal{E}}$ in Eq. (20), namely, $\omega_c + \delta_0 \cos(\omega_m t)$, which is just the desired frequency sweep of $2\delta_0$ in time π/ω_m.

There are certain requirements for ARP to occur efficiently. First, Ω must be large enough so that $\mathbf{R}$ precesses about $\mathbf{\Omega}'$ much faster than $\mathbf{\Omega}'$ rotates during the sweep, which means that $\Omega \gg \dot{\delta}/\Omega = \beta\omega_m^2/\Omega$ [see Eq. (20)]. This adiabatic following of $\mathbf{\Omega}'$ by $\mathbf{R}$ produces the "A" in ARP. For a uniform sweep rate, $\dot{\delta} = 2\delta_0\omega_m/\pi$, where $\pm\delta_0$ is the sweep range. So adiabaticity requires $\omega_m \ll \pi\Omega^2/2\delta_0$.

Second, the entire sweep must occur in a time that is short compared with the atomic excited-state lifetime to minimize the effects of spontaneous emission during the sweep and thereby preserve coherence between the atom and the radiation field. This requires $\omega_m \gg \gamma$, or $\dot{\delta} \gg 2\delta_0\gamma/\pi$, and constitutes the rapid condition in the name ARP. These are two conditions on the sweep time and the Rabi frequency Ω that must be met independently, in addition to their combination $\Omega \gg \gamma$.

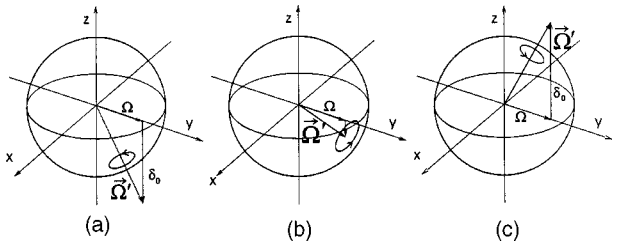

Fig. 18. At the beginning of the frequency sweep with the atoms in the ground state (south pole), the initial detuning δ_0 is much larger than the Rabi frequency Ω. Thus $\mathbf{R}$ executes small, rapid orbits near the south pole because the torque vector $\mathbf{\Omega}'$ is nearly polar as shown in part (a). As shown in part (b), $\delta = 0$, $\mathbf{R}$ executes orbits in a vertical plane because the only remaining component of the torque vector $\mathbf{\Omega}'$ is Ω, and thus $\mathbf{\Omega}'$ is in the equatorial plane. Near the end of the sweep δ is again very large, $\mathbf{R}$ orbits near the north pole as shown in part (c), and is finally left at the north pole with the atom in the excited state. Atoms that start at the north pole (excited state) are similarly driven in this coherent way to the south pole.

Finally, it is required that $\delta_0 \gg \Omega$, so that $\mathbf{\Omega}'$ is nearly polar at the extremes of the sweep. Thus δ_0 is the highest frequency in the system. All these conditions can be written together as

$$\gamma\sqrt{\beta} \ll \omega_m\sqrt{\beta} \ll \Omega \ll \delta_0. \quad (21)$$

The ARP force on He* has been measured by recording the atomic spatial distribution after deflection by appropriate transverse laser beams (see Refs. 84 and 89). The average measured velocity change was $3.8\ \gamma/k$, corresponding to a force of $3.8\,F_{\mathrm{rad}}$, about 3/5 of the prediction of the model. The velocity range of this measured force was $\sim\pm 3.8\gamma/k$, corresponding to $\sim 7.6 v_c$, considerably larger than that for F_{rad}. Even though the ARP conditions of Eq. (21) are not very well fulfilled in the measurements of Ref. 84, the observed force was $\gg F_{\mathrm{rad}}$ and had a magnitude comparable with the simple ARP model.

D. Summary

The ARP and bichromatic forces share many similarities in spite of their very different model descriptions. Both arise from controlled momentum transfer between modulated counterpropagating laser beams; the ARP force makes use of frequency-modulated light, while the bichromatic force relies on amplitude modulation. Although the physical models presented in the previous sections give predictions for the optimum parameters for the counterpropagating laser beams, in both experiment and calculation, for both the ARP force and the bichromatic force the strongest force is observed under conditions that do not satisfy their respective models.

6. CONCLUSIONS

In this paper we have reviewed some of the fundamentals of optical control of atomic motion. In addition, we have chosen a few broad areas to discuss in more detail. The reader is cautioned that this is by no means an exhaus-

tive review of the field and that many important and current topics have been omitted.

In place of a comprehensive (book-length) paper, we have simply selected a few special defining characteristics as a focus for discussion of several specific topics and then specialized to a few topics in domains where these characteristics do not apply (see Table 1). As we wrote in Subsection 1.C, we considered the characteristics of quantum states of atomic motion instead of classical trajectories for atoms, multilevel instead of two-level atoms, and polychromatic instead of monochromatic light. Each of these are subfields, along with many others, of this burgeoning field of controlling the motion of free, neutral atoms.

REFERENCES

1. H. J. Metcalf and P. van der Straten, *Laser Cooling and Trapping* (Springer-Verlag, New York, 1999).
2. W. Phillips and H. Metcalf, "Laser deceleration of an atomic beam," Phys. Rev. Lett. **48**, 596–599 (1982).
3. J. Prodan, W. Phillips, and H. Metcalf, "Laser production of a very slow monoenergetic atomic beam," Phys. Rev. Lett. **49**, 1149–1153 (1982).
4. J. Prodan and W. Phillips, "Chirping the light fantastic?—recent NBS atom cooling experiments," Prog. Quantum Electron. **8**, 231–235 (1984).
5. W. Ertmer, R. Blatt, J. L. Hall, and M. Zhu, "Laser manipulation of atomic beam velocities: demonstration of stopped atoms and velocity reversal," Phys. Rev. Lett. **54**, 996–999 (1985).
6. R. Watts and C. Wieman, "Manipulating atomic velocities using diode lasers," Opt. Lett. **11**, 291–293 (1986).
7. V. Bagnato, G. Lafyatis, A. Martin, E. Raab, R. Ahmad-Bitar, and D. Pritchard, "Continuous stopping and trapping of neutral atoms," Phys. Rev. Lett. **58**, 2194–2197 (1987).
8. T. E. Barrett, S. W. Dapore-Schwartz, M. D. Ray, and G. P. Lafyatis, "Slowing atoms with (σ^-)-polarized light," Phys. Rev. Lett. **67**, 3483–3487 (1991).
9. P. A. Molenaar, P. van der Straten, H. G. M. Heideman, and H. Metcalf, "Diagnostic technique for Zeeman-compensated atomic-beam slowing—technique and results," Phys. Rev. A **55**, 605–614 (1997).
10. J. Dalibard and W. Phillips, "Stability and damping of radiation pressure traps," Bull. Am. Phys. Soc. **30**, 748 (1985).
11. S. Chu, L. Hollberg, J. Bjorkholm, A. Cable, and A. Ashkin, "Three-dimensional viscous confinement and cooling of atoms by resonance radiation pressure," Phys. Rev. Lett. **55**, 48–51 (1985).
12. B. Sheehy, S. Q. Shang, P. van der Straten, and H. Metcalf, "Collimation of a rubidium beam below the Doppler limit," Chem. Phys. **145**, 317–325 (1990).
13. P. Gould, P. Lett, and W. D. Phillips, "New measurement with optical molasses," in *Laser Spectroscopy VIII*, W. Persson and S. Svanberg, eds. (Springer-Verlag, Berlin, 1987), pp. 64–00.
14. T. Hodapp, C. Gerz, C. Westbrook, C. Furtlehner, and W. Phillips, "Diffusion in optical molasses," Bull. Am. Phys. Soc. **37**, 1139 (1992).
15. P. Lett, R. Watts, C. Westbrook, W. Phillips, P. Gould, and H. Metcalf, "Observation of atoms laser cooled below the Doppler limit," Phys. Rev. Lett. **61**, 169–172 (1988).
16. P. D. Lett, R. N. Watts, C. E. Tanner, S. L. Rolston, W. D. Phillips, and C. I. Westbrook, "Optical molasses," J. Opt. Soc. Am. B **6**, 2084–2107 (1989).
17. A. Ashkin, "Acceleration and trapping of particles by radiation pressure," Phys. Rev. Lett. **24**, 156–159 (1970).
18. S. Chu, J. Bjorkholm, A. Ashkin, and A. Cable, "Experimental observation of optically trapped atoms," Phys. Rev. Lett. **57**, 314–317 (1986).
19. A. Ashkin, "Application of laser radiation pressure," Science **210**, 1081–1088 (1980).
20. A. Ashkin and J. M. Dziedzic, "Observation of radiation-pressure trapping of particles by alternating light beams," Phys. Rev. Lett. **54**, 1245–1248 (1985).
21. A. Ashkin and J. M. Dziedzic, "Optical trapping and manipulation of viruses and bacteria," Science **235**, 1517–1520 (1987).
22. J. D. Miller, R. A. Cline, and D. J. Heinzen, "Far-off-resonance optical trapping of atoms," Phys. Rev. A **47**, R4567–R4570 (1993).
23. C. S. Adams, H. J. Lee, N. Davidson, M. Kasevich, and S. Chu, "Evaporative cooling in a crossed dipole trap," Phys. Rev. Lett. **74**, 3577–3580 (1995).
24. T. Takekoshi and R. J. Knize, "CO_2-laser trap for cesium atoms," Opt. Lett. **21**, 77–79 (1996).
25. H. Metcalf and W. Phillips, "Electromagnetic trapping of neutral atoms," Metrologia **22**, 271–278 (1986).
26. N. Davidson, H. J. Lee, C. S. Adams, M. Kasevich, and S. Chu, "Long atomic coherence times in an optical dipole trap," Phys. Rev. Lett. **74**, 1311–1314 (1995).
27. A. Siegman, *Lasers* (University Sciences, Mill Valley, Calif., 1986).
28. N. Simpson, K. Dholakia, L. Allen, and M. Padgett, "The mechanical equivalence of spin and orbital angular momentum of light: an optical spanner," Opt. Lett. **22**, 52–54 (1997).
29. D. McGloin, N. Simpson, and M. Padgett, "Transfer of orbital angular momentum from a stressed fiber optic waveguide to a light beam," Appl. Opt. **37**, 469–472 (1998).
30. M. Beijersbergen, "Phase singularities in optical beams," Ph.D. thesis (Leiden University, Leiden, The Netherlands, 1996).
31. Yu. B. Ovchinnikov, I. Manek, and R. Grimm, "Surface trap for Cs atoms based on evanescent-wave cooling," Phys. Rev. Lett. **79**, 2225–2228 (1997).
32. C. G. Aminoff, A. M. Steane, P. Bouyer, P. Desbiolles, J. Dalibard, and C. Cohen-Tannoudji, "Cesium atoms bouncing in a stable gravitational cavity," Phys. Rev. Lett. **71**, 3083–3086 (1993).
33. M. A. Kasevich, D. S. Weiss, and S. Chu, "Normal-incidence reflection of slow atoms from an optical evanescent wave," Opt. Lett. **15**, 607–609 (1990).
34. A. Aspect, E. Arimondo, R. Kaiser, N. Vansteenkiste, and C. Cohen-Tannoudji, "Laser cooling below the one-photon recoil energy by velocity-selective coherent population trapping," Phys. Rev. Lett. **61**, 826–829 (1988).
35. F. Bardou, J. P. Bouchaud, O. Emile, A. Aspect, and C. Cohen-Tannoudji, "Subrecoil laser cooling and Levy flights," Phys. Rev. Lett. **72**, 203–206 (1994).
36. J. Hack, L. Liu, M. Olshanii, and H. Metcalf, "Velocity-selective coherent population trapping of two-level atoms," Phys. Rev. A **62**, 013405 (2000).
37. A. Aspect, C. Cohen-Tannoudji, E. Arimondo, N. Vansteenkiste, and R. Kaiser, "Laser cooling below the one-photon recoil energy by velocity-selective coherent population trapping—theoretical analysis," J. Opt. Soc. Am. B **6**, 2112–2124 (1989).
38. H. Batelaan, E. Rasel, M. Oberthaler, J. Schmeidmayer, and A. Zeilinger, "Classical and quantum atom fringes," in *Atom Interferometry*, P. Berman, ed. (Academic, New York, 1997), pp. 85–120.
39. E. Arimondo, "Velocity-selective coherent population trapping in one and two dimensions," in *Laser Manipulation of Atoms and Ions, Proceedings of the International School of Physics "Enrico Fermi," Course CXVII*, E. Arimondo, W. Phillips, and F. Strumia, eds. (North Holland, Amsterdam, 1991), pp. 191–224.
40. G. Morigi, B. Zambon, N. Leinfellner, and E. Arimondo, "Scaling laws in velocity-selective coherent-population-trapping laser cooling," Phys. Rev. A **53**, 2616–2626 (1996).
41. D. Bouwmeester, A. Ekert, and A. Zeilinger, *The Physics of Quantum Information* (Springer-Verlag, Berlin, 2000).
42. C. Monroe, "Quantum information processing with atoms and photons," Nature **416**, 238–246 (2002).
43. V. S. Letokhov, "Narrowing of the Doppler width in a standing light wave," JETP Lett. **7**, 272 (1968).

44. C. Salomon, J. Dalibard, A. Aspect, H. Metcalf, and C. Cohen-Tannoudji, "Channeling atoms in a laser standing wave," Phys. Rev. Lett. **59**, 1659–1662 (1987).
45. Y. Castin and J. Dalibard, "Quantization of atomic motion in optical molasses," Europhys. Lett. **14**, 761–766 (1991).
46. P. Verkerk, B. Lounis, C. Salomon, C. Cohen-Tannoudji, J. Y. Courtois, and G. Grynberg, "Dynamics and spatial order of cold cesium atoms in a periodic optical potential," Phys. Rev. Lett. **68**, 3861–3864 (1992).
47. P. S. Jessen, C. Gerz, P. D. Lett, W. D. Phillips, S. L. Rolston, R. J. C. Spreeuw, and C. I. Westbrook, "Observation of quantized motion of Rb atoms in an optical field," Phys. Rev. Lett. **69**, 49–52 (1992).
48. B. Lounis, P. Verkerk, J. Y. Courtois, C. Salomon, and G. Grynberg, "Quantized atomic motion in 1D cesium molasses with magnetic field," Europhys. Lett. **21**, 13–17 (1993).
49. R. Gupta, S. Padua, C. Xie, H. Batelaan, T. Bergeman, and H. Metcalf, "Motional quantization of laser cooled atoms," Bull. Am. Phys. Soc. **37**, 1139 (1992).
50. R. Gupta, S. Padua, T. Bergeman, and H. Metcalf, "Search for motional quantization of laser-cooled atoms," in *Laser Manipulation of Atoms and Ions, Proceedings of the International School of Physics "Enrico Fermi," Course CXVIII*, E. Arimondo, W. Phillips, and F. Strumia, eds. (North Holland, Amsterdam, 1991), pp. 345–360.
51. B. P. Anderson and M. A. Kasevich, "Macroscopic quantum interference from atomic tunnel arrays," Nature **282**, 1686–1689 (1998).
52. M. Greiner, O. Mandel, T. Esslinger, T. W. Hänsch, and I. Bloch, "Quantum phase transition from a superfluid to a Mott insulator in a gas of ultracold atoms," Nature **415**, 39–44 (2002).
53. G. Grynberg, B. Lounis, P. Verkerk, J. Y. Courtois, and C. Salomon, "Quantized motion of cold cesium atoms in 2-dimensional and 3-dimensional optical potentials," Phys. Rev. Lett. **70**, 2249–2252 (1993).
54. G. Birkl, M. Gatzke, I. H. Deutsch, S. L. Rolston, and W. D. Phillips, "Bragg scattering from atoms in optical lattices," Phys. Rev. Lett. **75**, 2823–2826 (1995).
55. C. I. Westbrook, R. N. Watts, C. E. Tanner, S. L. Rolston, W. D. Phillips, P. D. Lett, and P. L. Gould, "Localization of atoms in a 3-dimensional standing wave," Phys. Rev. Lett. **65**, 33–36 (1990).
56. M. Ben Dahan, E. Peik, J. Reichel, Y. Castin, and C. Salomon, "Bloch oscillations of atoms in an optical potential," Phys. Rev. Lett. **76**, 4508–4511 (1996).
57. J. Dalibard and C. Cohen-Tannoudji, "Laser cooling below the Doppler limit by polarization gradients—simple theoretical models," J. Opt. Soc. Am. B **6**, 2023–2045 (1989).
58. P. J. Ungar, D. S. Weiss, S. Chu, and E. Riis, "Optical molasses and multilevel atoms—theory," J. Opt. Soc. Am. B **6**, 2058–2071 (1989).
59. C. Cohen-Tannoudji and W. D. Phillips, "New mechanisms for laser cooling," Phys. Today **43**(10), 33–40 (1990).
60. R. Gupta, S. Padua, C. Xie, H. Batelaan, and H. Metcalf, "Simplest atomic system for sub-Doppler laser cooling," J. Opt. Soc. Am. B **11**, 537–541 (1994).
61. C. Salomon, J. Dalibard, W. D. Phillips, A. Clairon, and S. Guellati, "Laser cooling of cesium atoms below 3 μK," Europhys. Lett. **12**, 683–688 (1990).
62. J. Dalibard, C. Salomon, A. Aspect, E. Arimondo, N. Vansteenkiste, and C. Cohen-Tannoudji, "New schemes in laser cooling," in *Atomic Physics XI*, S. Haroche, J.-C. Gay, and G. Grynberg, eds. (World Scientific, Singapore, 1989), pp. 199–214.
63. B. Sheehy, S. Q. Shang, P. van der Straten, S. Hatamian, and H. Metcalf, "Magnetic-field-induced laser cooling below the Doppler limit," Phys. Rev. Lett. **64**, 858–861 (1990).
64. W. Ketterle and N. J. Vandruten, "Evaporative cooling of trapped atoms," Adv. Atom. Mol. Opt. Phys. **37**, 181–236 (1996).
65. M. Kasevich and S. Chu, "Laser cooling below a photon recoil with 3-level atoms," Phys. Rev. Lett. **69**, 1741–1744 (1992).
66. E. Raab, M. Prentiss, A. Cable, S. Chu, and D. Pritchard, "Trapping of neutral-sodium atoms with radiation pressure," Phys. Rev. Lett. **59**, 2631–2634 (1987).
67. H. Metcalf, "Magneto-optical trapping and its application to helium metastables," J. Opt. Soc. Am. B **6**, 2206–2210 (1989).
68. P. Molenaar, "Photoassociative reactions of laser-cooled sodium," Ph.D. thesis (Utrecht University, Utrecht, The Netherlands, 1995).
69. E. A. Cornell, C. Monroe, and C. E. Wieman, "Multiply loaded, ac magnetic trap for neutral atoms," Phys. Rev. Lett. **67**, 2439–2442 (1991).
70. A. M. Steane and C. J. Foot, "Laser cooling below the Doppler limit in a magnetooptical trap," Europhys. Lett. **14**, 231–236 (1991).
71. A. M. Steane, M. Chowdhury, and C. J. Foot, "Radiation force in the magnetooptical trap," J. Opt. Soc. Am. B **9**, 2142–2158 (1992).
72. T. Walker, D. Sesko, and C. Wieman, "Collective behavior of optically trapped neutral atoms," Phys. Rev. Lett. **64**, 408–411 (1990).
73. D. W. Sesko, T. G. Walker, and C. E. Wieman, "Behavior of neutral atoms in a spontaneous force trap," J. Opt. Soc. Am. B **8**, 946–958 (1991).
74. K. E. Gibble, S. Kasapi, and S. Chu, "Improved magnetooptic trapping in a vapor cell," Opt. Lett. **17**, 526–528 (1992).
75. K. Lindquist, M. Stephens, and C. Wieman, "Experimental and theoretical study of the vapor-cell Zeeman optical trap," Phys. Rev. A **46**, 4082–4090 (1992).
76. W. Ketterle, K. B. Davis, M. A. Joffe, A. Martin, and D. E. Pritchard, "High densities of cold atoms in a dark spontaneous-force optical trap," Phys. Rev. Lett. **70**, 2253–2256 (1993).
77. J. Söding, R. Grimm, Yu. B. Ovchinnikov, P. Bouyer, and C. Salomon, "Short-distance atomic-beam deceleration with a stimulated light force," Phys. Rev. Lett. **78**, 1420–1423 (1997).
78. R. Grimm, Yu. B. Ovchinnikov, A. I. Sidorov, and V. S. Letokhov, "Observation of a strong rectified dipole force in a bichromatic standing light wave," Phys. Rev. Lett. **65**, 1415–1418 (1990).
79. R. Gupta, C. Xie, S. Padua, H. Batelaan, and H. Metcalf, "Bichromatic laser cooling in a 3-level system," Phys. Rev. Lett. **71**, 3087–3090 (1993).
80. M. Cashen, O. Rivoire, V. Romanenko, L. Yatsenko, and H. Metcalf, "Strong optical forces in frequency-modulated light," Phys. Rev. A **64**, 063411 (2001).
81. M. Williams, F. Chi, M. Cashen, and H. Metcalf, "Measurement of the bichromatic optical force on Rb atoms," Phys. Rev. A **60**, R1763–R1766 (1999).
82. M. Williams, F. Chi, M. Cashen, and H. Metcalf, "Bichromatic force measurements using atomic beam deflections," Phys. Rev. A **61**, 023408 (2000).
83. M. Cashen and H. Metcalf, "Bichromatic force on helium," Phys. Rev. A **63**, 025406 (2001).
84. M. Cashen, O. Rivoire, L. Yatsenko, and H. Metcalf, "Coherent exchange of momentum between atoms and light," J. Opt. B **4**, 75–79 (2002).
85. A. Goepfert, I. Bloch, D. Haubrich, F. Lison, R. Schütze, R. Wynands, and D. Meschede, "Stimulated focusing and deflection of an atomic beam using picosecond laser pulses," Phys. Rev. A **56**, R3354–R3357 (1997).
86. R. Grimm, J. Söding, and Yu. B. Ovchinnikov, "Coherent beam splitter for atoms based on a bichromatic standing light wave," Opt. Lett. **19**, 658–660 (1994).
87. R. Grimm, G. Wasik, J. Söding, and Yu. B. Ovchinnikov, "Laser cooling and trapping with rectified optical dipole forces," in *Coherent and Collective Interactions of Particle Beams*, *Proceedings of the International School of Physics "Enrico Fermi," Course CXXXI*, A. Aspect, W. Barletta, and R. Bonifacio, eds. (IOS, Amsterdam, 1996), pp. 481–502.
88. E. Kyrola and S. Stenholm, "Velocity tuned resonances as multi-Doppleron processes," Opt. Commun. **22**, 123–126 (1977).
89. M. Cashen and H. Metcalf, "Optical forces on atoms in nonmonochromatic light," J. Opt. Soc. Am. B **20**, 915–924 (2003).

90. I. Nebenzahl and A. Szoke, "Deflection of atomic beams by resonance radiation using stimulated emission," Appl. Phys. Lett. **25**, 327–329 (1974).
91. V. Voitsekovich, M. Danileiko, A. Negriiko, V. Romanenko, and L. Yatsenko, "Pressure of light on atoms in the field of frequency-modulated waves," Ukr. Fiz. Zh. (Russ. Ed.) **36**, 192–197 (1991).
92. G. Demeter, G. Djotyan, and J. Bakos, "Deflection and splitting of atomic beams with counterpropagating, short, chirped laser pulses," J. Opt. Soc. Am. B **15**, 16–24 (1998).
93. R. Feynman, F. Vernon, and R. Hellwarth, "Geometrical representation of the Schrödinger equation for solving maser problems," J. App. Phys. **28**, 49–52 (1957).
94. L. Allen and J. H. Eberly, *Optical Resonance and Two-Level Atoms* (Dover, New York, 1975).